Physics Letters B 778 (2018) 101–127

Contents lists available at ScienceDirect

Physics Letters B

www.elsevier.com/locate/physletb

Search for Higgs boson pair production in events with two bottom quarks and two tau leptons in proton–proton collisions at $\sqrt{s} = 13\,\text{TeV}$

The CMS Collaboration *

CERN, Switzerland

ARTICLE INFO

Article history:
Received 10 July 2017
Received in revised form 28 December 2017
Accepted 1 January 2018
Available online 9 January 2018
Editor: M. Doser

Keywords:
CMS
Physics
Higgs
Higgs boson pair production

ABSTRACT

A search for the production of Higgs boson pairs in proton–proton collisions at a centre-of-mass energy of 13 TeV is presented, using a data sample corresponding to an integrated luminosity of $35.9\,\text{fb}^{-1}$ collected with the CMS detector at the LHC. Events with one Higgs boson decaying into two bottom quarks and the other decaying into two τ leptons are explored to investigate both resonant and nonresonant production mechanisms. The data are found to be consistent, within uncertainties, with the standard model background predictions. For resonant production, upper limits at the 95% confidence level are set on the production cross section for Higgs boson pairs as a function of the hypothesized resonance mass and are interpreted in the context of the minimal supersymmetric standard model. For nonresonant production, upper limits on the production cross section constrain the parameter space for anomalous Higgs boson couplings. The observed (expected) upper limit at 95% confidence level corresponds to about 30 (25) times the prediction of the standard model.

1. Introduction

The discovery of the Higgs boson (H) by the ATLAS and CMS Collaborations [1–3] was a major step towards improving the understanding of the mechanism of electroweak symmetry breaking (EWSB). With the mass of the Higgs boson now precisely determined [4], the structure of the Higgs scalar field potential and the Higgs boson self-couplings are precisely predicted in the standard model (SM). While the measured properties of the Higgs boson are thus far consistent with the expectations from the SM [5], the measurement of the Higgs boson self-coupling provides an independent test of the SM and verification that the Higgs mechanism is truly responsible for the EWSB by giving access to the shape of the Higgs scalar field potential [6].

The trilinear self-coupling of the Higgs boson (λ_{HHH}) can be extracted from the measurement of the Higgs boson pair (HH) production cross section. In the SM, for proton–proton (pp) collisions at the CERN LHC, this process occurs mainly via gluon–gluon fusion and involves either couplings of the Higgs boson to virtual fermions in a quantum loop, or the λ_{HHH} coupling itself, with the two processes interfering destructively as illustrated in Fig. 1.

The SM prediction for the cross section is $\sigma_{\text{HH}} = 33.49^{+4.3\%}_{-6.0\%}\,(\text{scale}) \pm 5.9\%\,(\text{theo})\,\text{fb}$ [7–11]. This value was computed at the next-to-next-to-leading order (NNLO) of the theoretical perturbative quantum chromodynamics (QCD) calculation, including next-to-next-to-leading-logarithm (NNLL) corrections and finite top quark mass effects at next-to-leading order (NLO). The theoretical uncertainties in σ_{HH} include uncertainties in the QCD factorization and renormalization scales, the strong coupling parameter α_S, parton distribution functions (PDF), and unknown effects from the finite top quark mass at NNLO.

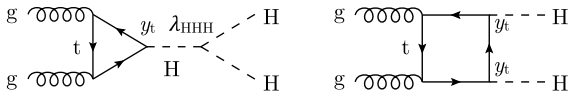

Fig. 1. Feynman diagrams contributing to Higgs pair production via gluon–gluon fusion at leading order at the LHC.

Beyond the standard model (BSM) physics effects can appear either via anomalous couplings of the Higgs boson or via new particles that can be directly produced or contribute to the quantum loops responsible for HH production. The experimental signature would be an enhancement of the HH production cross section for a specific value of the invariant mass of the pair (resonant production) or over the whole invariant mass spectrum (nonresonant production).

Resonant double Higgs boson production is predicted by many extensions of the SM such as the singlet model [12–14], the two-Higgs-doublet model [15] and its realisation as the minimal su-

* *E-mail address:* cms-publication-committee-chair@cern.ch.

https://doi.org/10.1016/j.physletb.2018.01.001

persymmetric standard model (MSSM) [16,17], and models with warped extra dimensions (WED) [18,19]. Although the physics motivation and the phenomenology of these theoretical models are very different, the signal is represented by a CP-even scalar particle (S) decaying into a Higgs boson pair, with an intrinsic width that is often negligible with respect to the detector resolution.

In the nonresonant case, the BSM physics is modelled through an effective Lagrangian that extends the SM Lagrangian with dimension-6 operators [20]. Five Higgs boson couplings result from this parametrization: the Higgs boson coupling to the top quark, y_t, the trilinear coupling λ_{HHH}, and three additional couplings, denoted as c_2, c_{2g}, and c_g using the notation in Ref. [7], that represent, respectively, the interactions of a top quark pair with a Higgs boson pair, of a gluon pair with a Higgs boson pair, and of a gluon pair with a single Higgs boson. For simplicity, we investigate only anomalous y_t and λ_{HHH} couplings, while the other anomalous couplings are assumed to be zero, and parametrize the deviations from the SM values as $k_\lambda = \lambda_{HHH}/\lambda_{HHH}^{SM}$ and $k_t = y_t/y_t^{SM}$. Extension of these results to any combination of the couplings can be obtained by following the procedure detailed in Ref. [21]. These two couplings are currently largely unconstrained by experimental results, and deviations from the SM can be accommodated by the combined measurements of Higgs boson properties [5] depending on the particular assumptions made about the BSM physics contributions.

Previous searches for the production of Higgs boson pairs were performed by both the ATLAS [22,23] and CMS [24,25] Collaborations using the LHC data collected at $\sqrt{s} = 8$ and 13 TeV. The most sensitive upper limit at 95% confidence level (CL) on HH production corresponds to 43 times the rate predicted by the SM and is obtained from the combination of the $HH \to b\bar{b}\gamma\gamma$ and $HH \to b\bar{b}\tau^+\tau^-$ decay channels using data collected at $\sqrt{s} = 8$ TeV [26].

In this Letter we present a search for Higgs boson pair production in the final state where one Higgs boson decays to $b\bar{b}$ and the other decays to $\tau^+\tau^-$. For simplicity, we refer to this process as $HH \to bb\tau\tau$ in the following, omitting the quark and lepton charges. This process has a combined branching fraction of 7.3% for a Higgs boson mass of 125 GeV. Its sizeable branching fraction, together with the relatively small background contribution from other SM processes, makes this final state one of the most sensitive to HH production. Three final states of the τ lepton pair are considered: one of the two τ leptons is required to decay into hadrons and a neutrino (τ_h), while the other can decay either to the same final state, or into an electron (τ_e) or a muon (τ_μ) and neutrinos. Together, these three final states include about 88% of the decays of the $\tau\tau$ system and are the most sensitive ones for this search. The data sample analyzed corresponds to an integrated luminosity of 35.9 fb^{-1} collected in pp collisions at $\sqrt{s} = 13$ TeV.

The search described in this Letter improves on the previous $HH \to bb\tau\tau$ results [26] by including final states with a leptonic τ decay, improving the event categorization, introducing multivariate methods for the background rejection, and optimizing the event and object selection for the LHC collisions at $\sqrt{s} = 13$ TeV.

2. The CMS detector

The central feature of the CMS apparatus is a superconducting solenoid of 6 m internal diameter, providing a magnetic field of 3.8 T. Within the solenoid volume are a silicon pixel and strip tracker, a lead tungstate crystal electromagnetic calorimeter (ECAL), and a brass and scintillator hadron calorimeter (HCAL), each composed of a barrel and two endcap sections. Forward calorimeters extend the pseudorapidity coverage provided by the barrel and endcap detectors. Muons are detected in gas-ionization chambers embedded in the steel flux-return yoke outside the solenoid. Events of interest are selected using a two-tiered trigger system [27]. The first level, composed of custom hardware processors, uses information from the calorimeters and muon detectors to select events at a rate of around 100 kHz within a time interval of less than 4 μs. The second level, known as the high-level trigger, consists of a farm of processors running a version of the full event reconstruction software optimized for fast processing, and reduces the event rate to less than 1 kHz before data storage. A more detailed description of the CMS detector, together with a definition of the coordinate system used and the relevant kinematic variables, including pseudorapidity η and azimuthal angle φ, can be found in Ref. [28].

3. Modelling of physics processes

Simulated samples of resonant and nonresonant HH production via gluon–gluon fusion are generated at leading order (LO) precision with MadGraph5_aMC@NLO 2.3.2 [29]. In the case of resonant production, separate samples are generated for mass values of the resonance ranging from 250 to 900 GeV. In the case of nonresonant production, separate samples are generated for different values of the effective Lagrangian couplings, including the couplings predicted by the SM [21,30]. In the latter case, an event weight determined as a function of the generated HH pair kinematics is applied to these samples to model signals corresponding to additional points in the effective Lagrangian parametrization.

Backgrounds arising from $Z/\gamma^* \to \ell\ell$ and $W \to \ell\nu_\ell$ in association with jets (with $\ell = e, \mu, \tau$), diboson (WW, ZZ, and WZ), and SM single Higgs boson production are simulated with MadGraph5_aMC@NLO 2.3.2 at LO with MLM merging [31], while the single top and $t\bar{t}$ backgrounds are simulated at NLO precision with powheg 2.0 [32,33]. The NNPDF3.0 [34] PDF set is used. In order to increase the number of simulated events that satisfy the requirements detailed in Section 4, the inclusive simulation of the Z/γ^* and W processes is complemented by samples simulated in selected regions of multiplicity, flavour, and the transverse momentum scalar sum of the partons emitted at the matrix element level. Signal and background generators are interfaced with pythia 8.212 [35] with the tune CUETP8M1 [36] to simulate the multiparton, parton shower, and hadronization effects. The simulated events include multiple overlapping hadron interactions as observed in the data.

The $t\bar{t}$, $Z/\gamma^* \to \ell\ell$, $W \to \ell\nu_\ell$ and single top quark samples are normalized to their theoretical cross sections at NNLO precision [37–39], and the diboson samples are normalized to their cross section at NLO precision [40]. The single Higgs boson production cross section is computed at the NNLO precision of the QCD corrections and at the NLO precision of electroweak corrections [7, 41–44].

4. Object reconstruction and event selection

In order to reconstruct an $HH \to bb\tau\tau$ candidate event, it is necessary to identify the e, μ, and τ_h leptons, the jets originating from the two b quarks, and the missing transverse momentum vector $\vec{p}_T^{\,miss}$, defined as the projection onto the plane perpendicular to the beam axis of the negative vector sum of the momenta of all reconstructed particle-flow objects in an event. Its magnitude is referred to as p_T^{miss}.

The particle-flow (PF) event algorithm [45] reconstructs and identifies each individual particle (PF candidate) with an optimized combination of information from the various elements of the CMS detector. The momentum of the muons is obtained from the curvature of the corresponding track. The energy of electrons is de-

termined from a combination of the electron momentum at the primary interaction vertex, as determined by the tracker, the energy of the corresponding ECAL cluster, and the energy sum of all bremsstrahlung photons spatially compatible with originating from the electron track. The energy of charged hadrons is determined from a combination of their momentum measured in the tracker and the matching ECAL and HCAL energy deposits, corrected for zero-suppression effects and for the response function of the calorimeters to hadronic showers. Finally, the energy of neutral hadrons is obtained from the corresponding corrected ECAL and HCAL energies. Complex objects, such as τ_h, jets, and the $\vec{p}_T^{\,miss}$ vector, are reconstructed from PF candidates. For each event, hadronic jets are clustered from PF candidates with the infrared and collinear safe anti-k_T algorithm [46,47], operated with distance parameters of 0.4 and 0.8. These jets are denoted as "AK4" and "AK8" in the following. Leptons from b hadron decays within a jet are considered as constituents by the algorithm. The jet momentum is determined as the vectorial sum of all particle momenta in the jet, and is found in the simulation to be within 5 to 10% of the true momentum over the whole p_T spectrum and detector acceptance. The invariant mass of AK8 jets is obtained by applying the soft drop jet grooming algorithm [48,49], that iteratively decomposes the jet into subjets to remove the soft wide-angle radiation and mitigates the contribution from initial state radiation, underlying event, and multiple hadron scattering. Jet energy corrections are derived from the simulation, and are confirmed with in situ measurements using the energy balance of dijet, multijet, γ+jet, and leptonic Z+jet events [50,51]. The PF components of the jets are used to reconstruct τ_h candidates using the hadrons plus strips algorithm [52,53], combining either one or three charged particle tracks with clusters of photons and electrons to identify the decay mode of the τ lepton.

Events in the $bb\tau_\mu\tau_h$ ($bb\tau_e\tau_h$) final state have been recorded using a set of triggers that require the presence of a single muon (electron) in the event. The selected events are required to contain a reconstructed muon (electron) [54,55] of $p_T > 23(27)$ GeV and $|\eta| < 2.1$ and a reconstructed τ_h candidate [52] of $p_T > 20$ GeV and $|\eta| < 2.3$. The muon (electron) candidate must satisfy the relative isolation requirement $I^{rel} < 0.15\,(0.1)$ [54,55], while the τ_h candidate must satisfy the "medium" working point of a multivariate isolation discriminant [52], that corresponds to a signal efficiency of about 60% and a jet misidentification rate ranging between 0.1% and 1% depending on the jet p_T. The reconstructed tracks associated to the selected electron, muon, and τ_h candidates must be compatible with the primary pp interaction vertex of the event. Electrons and muons erroneously reconstructed as a τ_h candidate are rejected using discriminants based on the information from the calorimeters and muon detectors and on the properties of the PF candidates that form the τ_h candidate, as is detailed in [52].

A trigger requiring the presence of two τ_h candidates is used to record events in the $bb\tau_h\tau_h$ final state. The selected events must contain two reconstructed τ_h candidates with $p_T > 45$ GeV and $|\eta| < 2.1$, that are required to pass the "medium" working point of the multivariate isolation discriminant and whose associated tracks must be compatible with the primary pp interaction vertex of the event. The discriminants that suppress the contribution from prompt electrons and muons are applied to both τ_h candidates as in the $bb\tau_\mu\tau_h$ and $bb\tau_e\tau_h$ final states.

For all three final states, the two selected τ leptons are required to have opposite electric charge. Events containing additional isolated muons or electrons are rejected to reduce the $Z/\gamma^* \to \ell\ell$ background contribution.

Events selected with the criteria described above ($\tau_\mu\tau_h$, $\tau_e\tau_h$, $\tau_h\tau_h$) are required to have two additional AK4 jets with $p_T > 20$ GeV and $|\eta| < 2.4$. In the case of HH production via a resonance of mass 700 GeV or higher, the two jets originating from the $H \to bb$ decay partially overlap due to the high Lorentz boost of the Higgs boson, and are reconstructed at the same time as two separate AK4 jets and as a single AK8 jet. To profit from this information, the event is classified as "boosted" if it contains at least one AK8 jet of invariant mass larger than 30 GeV and $p_T > 170$ GeV that is composed of two subjets, each geometrically matched to one of the selected AK4 jets ($\Delta R(\text{AK4, subjet}) < 0.4$, where $\Delta R = \sqrt{(\Delta\eta)^2 + (\Delta\varphi)^2}$ denotes the spatial separation of the jet candidates). The event is classified as "resolved" if any of these requirements is not satisfied. This classification provides a clear separation of the signal topology against the $t\bar{t}$ background, where the two jets are typically more spatially separated and not reconstructed as a single AK8 jet. The AK8 jet mass requirement is applied to reject candidates resulting from a single quark or gluon hadronization or poorly reconstructed by the soft drop algorithm.

The combined secondary vertex [56] algorithm is applied to the selected jets to identify those originating from a bottom quark and reduce the contribution from the multijet background where jets are initiated by light quarks or gluon radiation. Both the "medium" and the "loose" working points of the b tagging discriminant [57] are used in this search as described below. The efficiency and rate of erroneous b jet identification are about 60%(80%) and 1%(10%) respectively for the "medium" ("loose") working point.

Jets reconstructed in events classified as "resolved" are defined as b-tagged if they satisfy the "medium" working point of the b tagging algorithm. These events are classified into two groups according to the number of b-tagged jets: the group with at least two b-tagged jets (2b) has the best sensitivity, and the group with exactly one b-tagged jet (1b1j) increases the signal acceptance. Both AK4 jets previously selected in the events classified as "boosted" are required to satisfy the "loose" working point of the b tagging discriminant.

5. Signal regions and discriminating observables

After the object selection and event classification, the kinematic information of the event is exploited to reduce the contribution from background processes. The invariant mass of the two τ lepton candidates, $m_{\tau\tau}$, is reconstructed using a dynamic likelihood technique called SVfit [58] that combines the kinematics of the two visible lepton candidates and the missing transverse momentum in the event. The bb invariant mass, m_{bb}, is estimated from the two selected jet candidates for "resolved" topologies and from the invariant mass of the AK8 jet for "boosted" topologies. In the "resolved" case, the events are required to satisfy the condition:

$$\frac{(m_{\tau\tau} - 116\,\text{GeV})^2}{(35\,\text{GeV})^2} + \frac{(m_{bb} - 111\,\text{GeV})^2}{(45\,\text{GeV})^2} < 1, \quad (1)$$

where the values of 35 and 45 GeV are related to the mass resolution of the $\tau\tau$ and bb systems and 116 and 111 GeV correspond to the position of the expected reconstructed 125 GeV Higgs boson peak in the $m_{\tau\tau}$ and m_{bb} distributions, respectively. The selection has been optimized for the SM HH process to obtain a signal efficiency of approximately 80% and a background reduction of about 85% in the most sensitive event categories. The m_{bb} peak is shifted below the Higgs boson mass value because the momenta of neutrinos from b hadron decays are not measured. This effect also prevents the SVfit algorithm from fully recovering the $\tau\tau$ system mass value. In the "boosted" case the events are required to satisfy:

$$\begin{aligned} &80 < m_{\tau\tau} < 152\,\text{GeV}, \\ &90 < m_{bb} < 160\,\text{GeV}. \end{aligned} \quad (2)$$

In addition to the previous requirements, a multivariate discriminant is applied to the events in the resolved categories of the $\mathrm{bb}\tau_\mu\tau_\mathrm{h}$ and $\mathrm{bb}\tau_\mathrm{e}\tau_\mathrm{h}$ final states to identify and reject the $\mathrm{t\bar{t}}$ process, which is the most important source of background. The discriminant is built using the boosted decision tree (BDT) [59,60] algorithm that is trained on a combination of $\tau_\mu\tau_\mathrm{h}$ and $\tau_\mathrm{e}\tau_\mathrm{h}$ simulated signal and background events. The algorithm identifies the kinematic differences between the two processes and assigns to every selected event a number that defines its compatibility with a signal or background topology. Two separate BDT trainings are performed to achieve an optimal performance for all the signal processes studied.

One training is performed using resonant signals with masses $m_\mathrm{S} \leq 350\,\mathrm{GeV}$ as input. Eight variables are used in the discriminant training because of their good separation between signal and background: $\Delta\varphi(\mathrm{H_{bb}}, \mathrm{H}_{\tau\tau})$, $\Delta\varphi(\mathrm{H}_{\tau\tau}, \vec{p}_\mathrm{T}^{\,\mathrm{miss}})$, $\Delta\varphi(\mathrm{H_{bb}}, \vec{p}_\mathrm{T}^{\,\mathrm{miss}})$, $\Delta R(\mathrm{b,b})\, p_\mathrm{T}(\mathrm{H_{bb}})$, $\Delta R(\ell, \tau_\mathrm{h})\, p_\mathrm{T}(\mathrm{H}_{\tau\tau})$, $m_\mathrm{T}(\ell)$, $m_\mathrm{T}(\tau_\mathrm{h})$, and $\Delta\varphi(\ell, \vec{p}_\mathrm{T}^{\,\mathrm{miss}})$. Here ℓ refers to the selected muon or electron, $\mathrm{H_{bb}}$ and $\mathrm{H}_{\tau\tau}$ denote the H boson candidates reconstructed from the two jets and the two τ leptons, respectively, and $m_\mathrm{T}(\ell) = \sqrt{(p_\mathrm{T}^\ell + p_\mathrm{T}^{\mathrm{miss}})^2 - (\vec{p}_\mathrm{T}^{\,\ell} + \vec{p}_\mathrm{T}^{\,\mathrm{miss}})^2}$ denotes the transverse mass of the selected lepton candidate, with a similar definition for $m_\mathrm{T}(\tau_\mathrm{h})$. The ΔR separations of the two b quarks and of the two tau leptons are multiplied by the $\mathrm{H_{bb}}$ and $\mathrm{H}_{\tau\tau}$ candidate p_T respectively to reduce their dependence on the m_S hypothesis. All the selected variables contribute significantly to the discrimination achieved with the trained BDT. The same training is used both for the search for resonant HH production up to $m_\mathrm{S} = 350\,\mathrm{GeV}$ and for the search for nonresonant HH production. No loss of performance is observed by using this training in comparison to a dedicated training on nonresonant signals. Different selections on the BDT discriminant output are applied in the two searches to maximize the sensitivity: these selections correspond to a rejection of the $\mathrm{t\bar{t}}$ background of approximately 90 and 70% for the resonant and nonresonant searches, respectively, for a signal efficiency ranging between 65 and 95% depending on the signal hypothesis considered.

A second training is performed on the resonant signals of mass $m_\mathrm{S} > 350\,\mathrm{GeV}$. The variables used as inputs to this training are the same as in the previous case, but replacing $\Delta R(\mathrm{b,b})\, p_\mathrm{T}(\mathrm{H_{bb}})$ and $\Delta R(\ell, \tau_\mathrm{h})\, p_\mathrm{T}(\mathrm{H}_{\tau\tau})$ with $\Delta R(\mathrm{b,b})$ and $\Delta R(\ell, \tau_\mathrm{h})$. The selection on the BDT output is chosen to maximize the sensitivity and corresponds to a rejection of the $\mathrm{t\bar{t}}$ background of approximately 90% for a signal efficiency ranging between 70 and 95% depending on the value of m_S. In the case of the resonant search, the selections applied to the two BDT discriminants define low-mass (LM) and high-mass (HM) signal regions.

In the resonant search, the invariant mass of the two visible τ lepton decay products and the two selected b jets is used to search for a possible signal above the expected background event distribution. In order to improve the resolution and to enhance the sensitivity of the analysis, the invariant mass is reconstructed using a kinematic fit ($m_\mathrm{HH}^\mathrm{KinFit}$) that is detailed in Ref. [61]. The fit is based on the four-momenta of the τ and b candidates and on the $\vec{p}_\mathrm{T}^{\,\mathrm{miss}}$ vector in the event, and is performed under the hypothesis of two 125 GeV Higgs bosons decaying into a bottom quark pair and a τ lepton pair. The use of the kinematic fit improves the resolution on m_HH by about a factor of two compared to the four-body invariant mass of the reconstructed leptons and jets.

The stransverse mass or m_T2 variable is used in the search for a nonresonant signal. This variable, originally introduced for supersymmetry searches involving invisible particles in the final state [62,63] and later proposed for HH searches in $\mathrm{bb}\tau\tau$ events [64], is used to reconstruct events where two equal mass particles are produced and each undergoes a two-body decay into a visible and an invisible particle. The m_T2 variable is defined as the largest mass of the parent particle that is compatible with the kinematic constraints of the event. In the case of the $\mathrm{bb}\tau\tau$ decay, where the dominant background is $\mathrm{t\bar{t}}$ production, the parent particle is interpreted as the top quark that decays into a bottom quark and a W boson. Following the description in Ref. [64], we denote with $\vec{b}$, $\vec{b}'$ the momenta of the two selected b jets and with m_b, $m_{b'}$ their invariant masses, and we introduce the $\vec{c}$, $\vec{c}\,'$ symbols to denote the momenta of the other particles produced in the top quark decay corresponding to the measured leptons and the neutrinos. We also set $m_c = m^\mathrm{vis}(\tau_1)$ and $m_{c'} = m^\mathrm{vis}(\tau_2)$, where m^vis denotes the invariant mass of the measured leptons or τ_h. Under this notation, m_T2 is defined as:

$$m_\mathrm{T2}\left(m_b, m_{b'}, \vec{b}_\mathrm{T}, \vec{b}'_\mathrm{T}, \vec{p}_\mathrm{T}^{\,\Sigma}, m_c, m_{c'}\right) = \min_{\vec{c}_\mathrm{T}+\vec{c}_\mathrm{T}'=\vec{p}_\mathrm{T}^{\,\Sigma}} \left\{\max\left(m_\mathrm{T}, m'_\mathrm{T}\right)\right\}, \tag{3}$$

where the constraint in the minimization is over the measured lepton momenta and the missing transverse momentum, i.e. $\vec{p}_\mathrm{T}^{\,\Sigma} = \vec{p}_\mathrm{T}^{\,\mathrm{vis}}(\tau_1) + \vec{p}_\mathrm{T}^{\,\mathrm{vis}}(\tau_2) + \vec{p}_\mathrm{T}^{\,\mathrm{miss}}$. In Eq. (3), the transverse mass m_T is defined as

$$m_\mathrm{T}\left(\vec{b}_\mathrm{T}, \vec{c}_\mathrm{T}, m_b, m_c\right) = \sqrt{m_b^2 + m_c^2 + 2\left(e_b e_c - \vec{b}_\mathrm{T}\cdot\vec{c}_\mathrm{T}\right)}, \tag{4}$$

and the "transverse energy" e of a particle of transverse momentum p_T and mass m is defined as

$$e = \sqrt{m^2 + p_\mathrm{T}^2}. \tag{5}$$

We use the implementation in Ref. [65] to perform the minimization of Eq. (3).

The m_T2 variable has a large discriminating power between the HH signal and the $\mathrm{t\bar{t}}$ background, as it is bounded above by the top quark mass m_t for the irreducible background process $\mathrm{t\bar{t}} \to \mathrm{bb\,WW} \to \mathrm{bb}\,\tau\nu_\tau\,\tau\nu_\tau$, while it can assume larger values for the HH signal where the tau and the b jet do not originate from the same parent particle. Detector resolution effects and other decay modes of the $\mathrm{t\bar{t}}$ system (e.g. jets from the W boson misidentified as τ_h) result in an extension of the tail of the m_T2 distribution in $\mathrm{t\bar{t}}$ events beyond the m_t value.

6. Background estimation

The main background sources that contaminate the signal region are $\mathrm{t\bar{t}}$ production, $\mathrm{Z}/\gamma^* \to \ell\ell$ production and QCD multijet events.

The backgrounds from $\mathrm{t\bar{t}}$, single top, single Higgs boson, W boson in association with jets, and diboson processes are estimated from simulation, as described in Section 3.

The $\mathrm{Z}/\gamma^* \to \ell\ell$ background contribution is estimated using the simulation, where the LO modelling of jet emission in the Z/γ^* process is known to be imperfect [66]. Therefore, correction factors are calculated using events containing two isolated, opposite-sign muons compatible with the $\mathrm{Z} \to \mu\mu$ decay in association with two jets that satisfy similar invariant mass criteria as in the signal region. This Z+2 jets sample is divided into three control regions according to the number of b-tagged jets (0, 1, and 2) and three correction factors are derived for the Z/γ^* production in association with 0, 1, or $\geq$2 generator level jets initiated by b quarks, and applied in the signal regions.

The multijet background is determined from data in a jet-enriched region defined by requiring that the two selected τ lepton candidates have the same electric charge. The yield is obtained

from this same-sign (SS) region, where all the other selections are applied as in the signal region. The events in this region are scaled by the ratio of opposite-sign (OS) to SS event yields obtained in a multijet-enriched region with inverted τ lepton isolation. The contributions of other backgrounds, based on predictions from simulated samples, are subtracted in the OS and SS regions. The shape of the multijet background is estimated using the events in an SS region with relaxed τ lepton isolation, after subtracting the other background contributions.

7. Systematic uncertainties

The effects of an imperfect knowledge of the detector response, discrepancies between simulation and data, and limited knowledge of the background and signal processes are accounted for in the analysis as systematic uncertainties. They are separately treated as "normalization" uncertainties or "shape" uncertainties; the first affect the number of expected events in the signal region, while the second affect their distributions.

7.1. Normalization uncertainties

The following normalization uncertainties are considered:

- The integrated luminosity is known with an uncertainty of 2.5% [67]. This value is obtained from dedicated Van der Meer scans and the stability of detector response during the data taking. The uncertainty is applied to the signal and to $\mathrm{t\bar{t}}$, W+jets, single top quark, single Higgs boson, and diboson backgrounds, but it is not applied to the multijet and Z+jets backgrounds because they are estimated or corrected from data.
- Electron, muon, and τ_h lepton trigger, reconstruction and identification efficiencies are measured using $\mathrm{Z} \to \mathrm{ee}$, $\mathrm{Z} \to \mu\mu$, and $\mathrm{Z} \to \tau\tau \to \tau_\mathrm{h}\nu_\tau\mu\nu_\mu\nu_\tau$ events collected at $\sqrt{s} = 13\,\mathrm{TeV}$. The corresponding uncertainties are considered as uncorrelated among the final states and are about 3% for electrons, 2% for muons, and 6% for τ leptons.
- The uncertainty in the knowledge of the τ_h energy scale is about 3% for each τ_h candidate [53], and its impact on the overall normalization ranges from 3 to 10% depending on the process being considered. This effect is fully correlated with a corresponding shape uncertainty in the distribution of m_{T2} and $m_{\mathrm{HH}}^{\mathrm{KinFit}}$.
- Uncertainties arising from the imperfect knowledge of the jet and b jet measured energy [50] have an impact of about 2% for the signal processes and 4% for the backgrounds.
- Uncertainties in the b tagging efficiency in the simulation are evaluated as functions of jet p_T and η [57] and result in an average value of 2 to 6% for the samples with genuine b jets in the final state.
- For the $\mathrm{t\bar{t}}$ process, the uncertainty in the normalization of the cross section is $+4.8\%/-5.5\%$. For the W+jets, single top quark, diboson, and single Higgs backgrounds, uncertainties range from 1 to 10%.
- The uncertainties in the three correction factors derived in the control regions with 0, 1, and 2 b-tagged jets for the $\mathrm{Z}/\gamma^* \to \ell\ell$ background are propagated from the control regions to the signal region, taking into account the correlation between them, and amount to an uncertainty in the range 0.1–2.5%
- The uncertainty in the multijet background normalization is estimated by propagating the statistical uncertainties in the number of events used for its determination in the region with the sign requirement inverted, as described in Section 6, and ranges between 5 and 30% depending on the final state and category. Additional sources of systematic uncertainties were found to be negligible with respect to the statistical component given the number of events in the signal and control regions.
- The uncertainties in the signal cross section arising from scale variations result in an uncertainty in its normalization of $+4.3\%/-6.0\%$ while effects from other theoretical uncertainties such as uncertainties on α_s, PDFs and finite top quark mass effects at NNLO amount to a further 5.9% uncertainty.

Table 1
Systematic uncertainties affecting the normalization of the different processes.

Systematic uncertainty	Value	Processes
Luminosity	2.5%	all but multijet, $\mathrm{Z}/\gamma^* \to \ell\ell$
Lepton trigger and reconstruction	2–6%	all but multijet
τ energy scale	3–10%	all but multijet
Jet energy scale	2–4%	all but multijet
b tag efficiency	2–6%	all but multijet
Background cross section	1–10%	all but multijet, $\mathrm{Z}/\gamma^* \to \ell\ell$
$\mathrm{Z}/\gamma^* \to \ell\ell$ SF uncertainty	0.1–2.5%	$\mathrm{Z}/\gamma^* \to \ell\ell$
Multijet normalization	5–30%	multijet
Scale unc.	$+4.3\%/-6.0\%$	signals
Theory unc.	5.9%	signals

The systematic uncertainties are summarized in Table 1.

7.2. Shape uncertainties

The following shape uncertainties are considered:

- The shape uncertainty affecting the kinematic distribution in the simulation of the $\mathrm{t\bar{t}}$ background is estimated by varying the top quark p_T distribution according to the uncertainties in differential p_T measurements described in Ref. [68], and has an impact smaller than 1% on the sensitivity of the measurement.
- Uncertainties due to the limited number of simulated events or due to the statistical fluctuations of events in the multijet control region are taken into account. These uncertainties are uncorrelated across bins in the individual template shapes and their inclusion has an impact on the sensitivity smaller than 7%.
- Uncertainties due to the τ_h and jet energy scales are taken into account and are fully correlated with the associated normalization uncertainties. Uncertainties in the energy scales for other objects have negligible impacts on the simulated event distributions and are not taken into account.

8. Results

Figs. 2, 3, and 4 show the distributions of the $m_{\mathrm{HH}}^{\mathrm{KinFit}}$ and m_{T2} variables in the $\tau_\mu\tau_\mathrm{h}$, $\tau_\mathrm{e}\tau_\mathrm{h}$, and $\tau_\mathrm{h}\tau_\mathrm{h}$ final states, respectively. The expected signature of resonant HH production is a localized excess in the $m_{\mathrm{HH}}^{\mathrm{KinFit}}$ distribution, while an enhancement in the tails of the m_{T2} distribution would reveal the presence of nonresonant HH production. A binned maximum likelihood fit is performed simultaneously in the signal regions defined in this search for the three final states considered. The systematic uncertainties discussed previously in Section 7 are introduced as nuisance parameters in the maximum likelihood fit. In the absence of evidence for a signal, we set 95% CL upper limits on the cross section for Higgs boson pair production using the asymptotic modified frequentist method (asymptotic $\mathrm{CL_s}$) [69,70].

For the resonant production mode, limits are set as a function of the mass of the resonance m_S under the hypothesis that

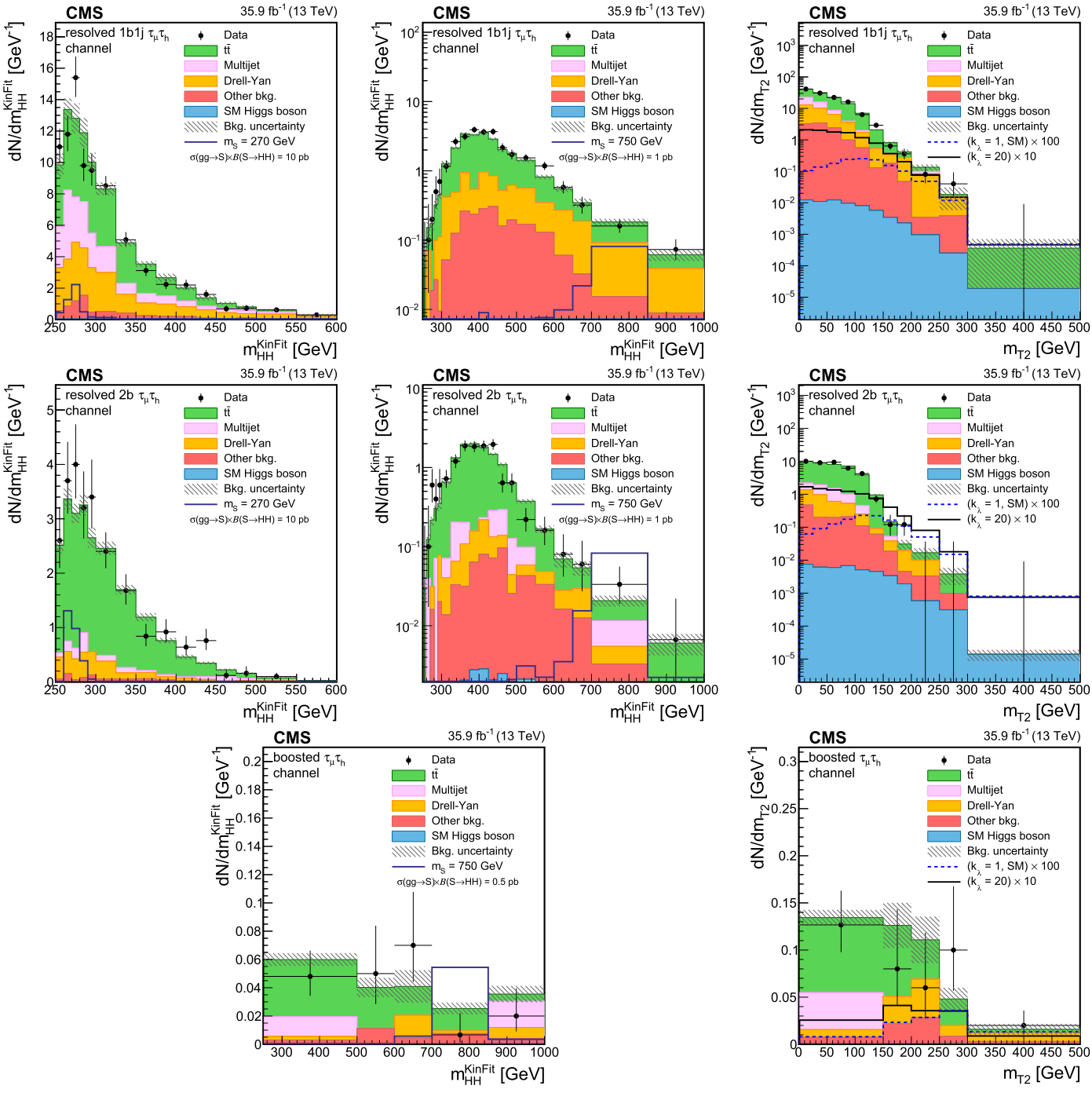

Fig. 2. Distributions of the events observed in the signal regions of the $\tau_\mu\tau_h$ final state. The first, second, and third rows show the resolved 1b1j, 2b, and boosted regions, respectively. Panels in the right column show the distribution of the m_{T2} variable, while the other panels show the distribution of the m_{HH}^{KinFit} variable, separated in the low-mass (LM, left panels) and high-mass (HM, central panels) regions for the resolved event categories. Data are represented by points with error bars and expected signal contributions are represented by the solid (BSM HH signals) and dashed (SM nonresonant HH signal) lines. Expected background contributions (shaded histograms) and associated systematic uncertainties (dashed areas) are shown as obtained after the maximum likelihood fit to the data under the background-only hypothesis. The background histograms are stacked while the signal histograms are not stacked.

its intrinsic width is negligible compared to the experimental resolution. The observed and expected 95% CL limits are shown in Fig. 5, upper panel. The figure also shows the expectation for radion production, a spin-0 state predicted in WED models, for the parameters $\Lambda_R = 3\,\text{TeV}$ (mass scale) and $kl = 35$ (size of the extra dimension), and assuming the absence of mixing with the Higgs boson. The corresponding cross section and branching fractions are taken from [71]. These model-independent limits are also interpreted in the hMSSM scenario [72,73], that is a parametrization of the MSSM that considers the observed 125 GeV Higgs boson as the lighter scalar predicted from the model (usually denoted as h in the context of the model), while the resonance of mass m_S represents the heavier CP-even scalar (usually denoted as H in the context of the model). Excluded regions as a function of the m_A and $\tan\beta$ parameters, representing respectively the mass of the CP-odd scalar and the ratio of the vacuum expectation values of the two Higgs doublets of the model, are shown in Fig. 5, lower panel. The minimum of the sensitivity around $m_S = 270\,\text{GeV}$ re-

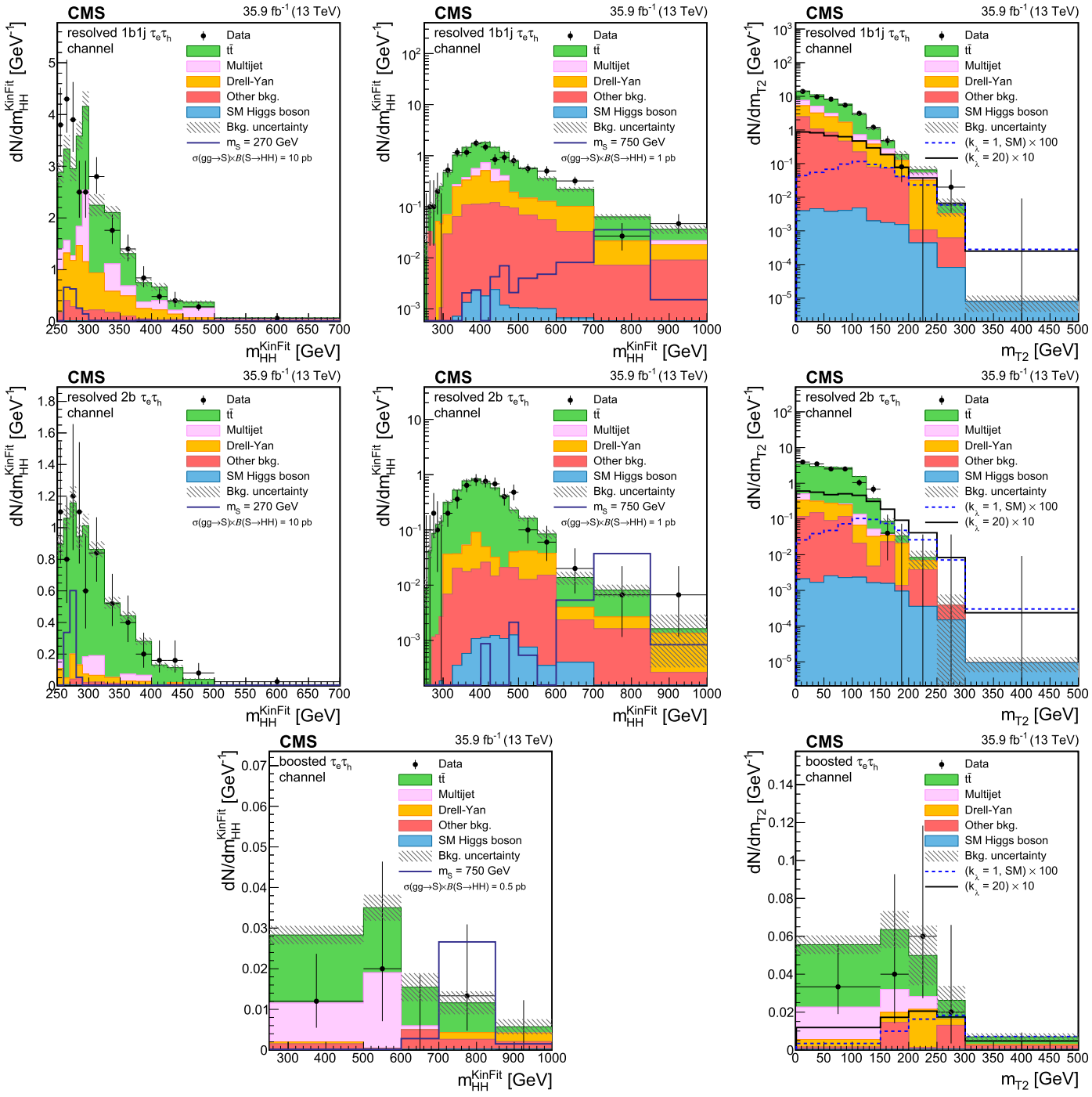

Fig. 3. Distributions of the events observed in the signal regions of the $\tau_e\tau_h$ final state. The first, second, and third rows show the resolved 1b1j, 2b, and boosted regions, respectively. Panels in the right column show the distribution of the m_{T2} variable, while the other panels show the distribution of the m_{HH}^{KinFit} variable, separated in the low-mass (LM, left panels) and high-mass (HM, central panels) regions for the resolved event categories. Data are represented by points with error bars and expected signal contributions are represented by the solid (BSM HH signals) and dashed (SM nonresonant HH signal) lines. Expected background contributions (shaded histograms) and associated systematic uncertainties (dashed areas) are shown as obtained after the maximum likelihood fit to the data under the background-only hypothesis. The background histograms are stacked while the signal histograms are not stacked.

sults in the presence of two separate expected excluded regions in this interpretation.

For the nonresonant production mode, including the theoretical uncertainties, the observed 95% CL upper limit on the HH production cross section times branching fraction amounts to 75.4 fb while the expected 95% CL upper limit amounts to 61.0 fb. These values correspond to about 30 and 25 times the SM prediction, respectively. Limits are set for different hypotheses of anomalous self-coupling and top quark coupling of the Higgs boson. The signal kinematics depend on the ratio of the two couplings and 95% CL upper limits are set as a function of k_λ/k_t, assuming the other BSM couplings to be zero. The result is shown in Fig. 6, upper panel, and the exclusion is compared with the theoretical prediction for the cross section for $k_t = 1$ and $k_t = 2$. The sensitivity varies as a function of k_λ and k_t because of the corresponding changes in the signal m_{T2} distribution. These upper limits are used

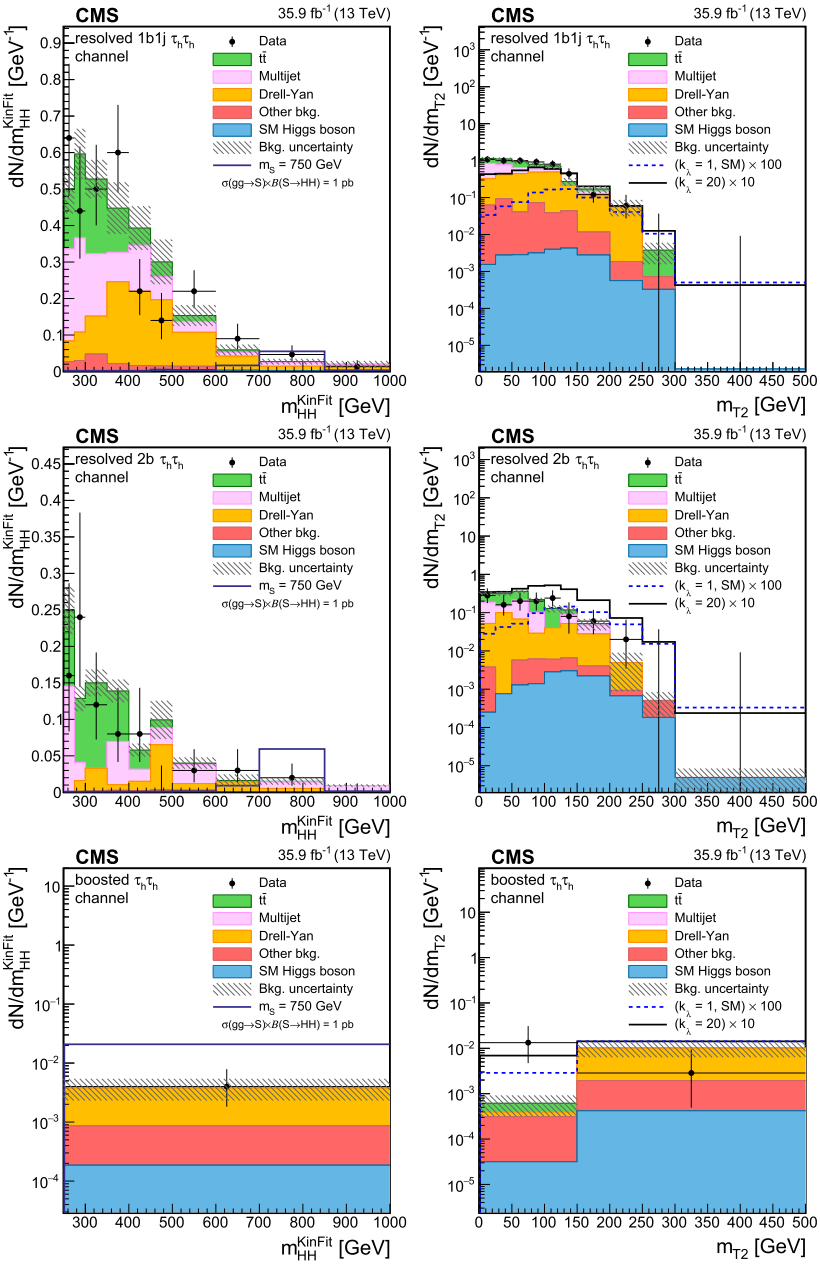

Fig. 4. Distributions of the events observed in the signal regions of the $\tau_h\tau_h$ final state. The first, second, and third rows show the resolved 1b1j, 2b, and boosted regions, respectively. Panels in the left column show the distribution of the m_{HH}^{KinFit} variable and panels in the right column show the distribution of the m_{T2} variable. Data are represented by points with error bars and expected signal contributions are represented by the solid (BSM HH signals) and dashed (SM nonresonant HH signal) lines. Expected background contributions (shaded histograms) and associated systematic uncertainties (dashed areas) are shown as obtained after the maximum likelihood fit to the data under the background-only hypothesis. The background histograms are stacked while the signal histograms are not stacked.

to set constraints on anomalous k_λ and k_t couplings as shown in Fig. 6, lower panel, where the c_2, c_{2g}, and c_g couplings are assumed to be equal to zero. The branching fractions for the decays of the Higgs boson into a bb and $\tau\tau$ pair are assumed to be those predicted by the SM for all the values of k_λ and k_t tested.

9. Summary

A search for resonant and nonresonant Higgs boson pair (HH) production in the bb$\tau\tau$ final state is presented. This search uses a data sample collected in proton–proton collisions at $\sqrt{s} = 13$ TeV that corresponds to an integrated luminosity of 35.9 fb^{-1}. The three most sensitive decay channels of the τ lepton pair, requiring the decay of one or both τ leptons into final-state hadrons and a neutrino, are used. The results are found to be statistically compatible with the expected standard model (SM) background contribution, and upper limits at the 95% confidence level are set on the HH production cross sections.

For the resonant production mechanism, upper exclusion limits at 95% confidence level (CL) are obtained for the production of a narrow resonance of mass m_S ranging from 250 to 900 GeV. These model-independent results are interpreted in the context of the hMSSM scenario, where a region in the parameter space corresponding to values of m_A between 230 and 360 GeV and $\tan\beta \lesssim 2$ is excluded at 95% CL.

For the nonresonant production mechanism, the theoretical framework of an effective Lagrangian is used to parametrize the

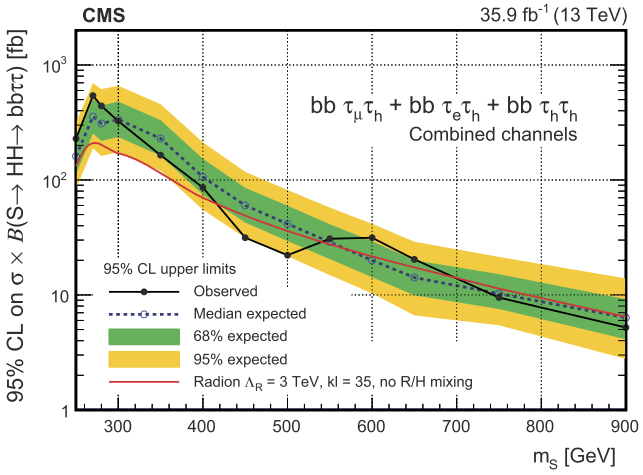

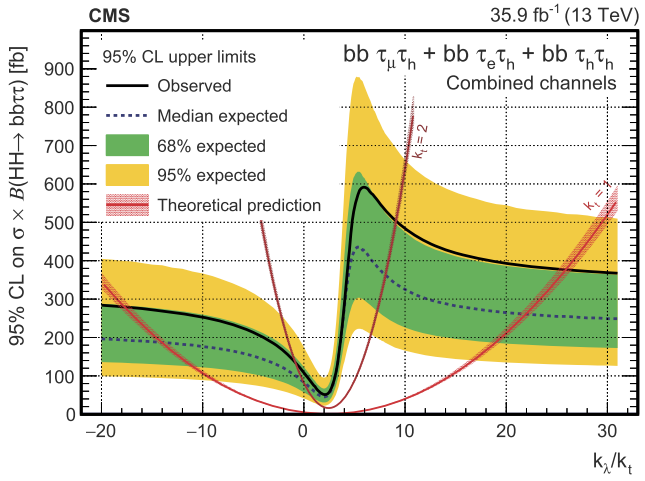

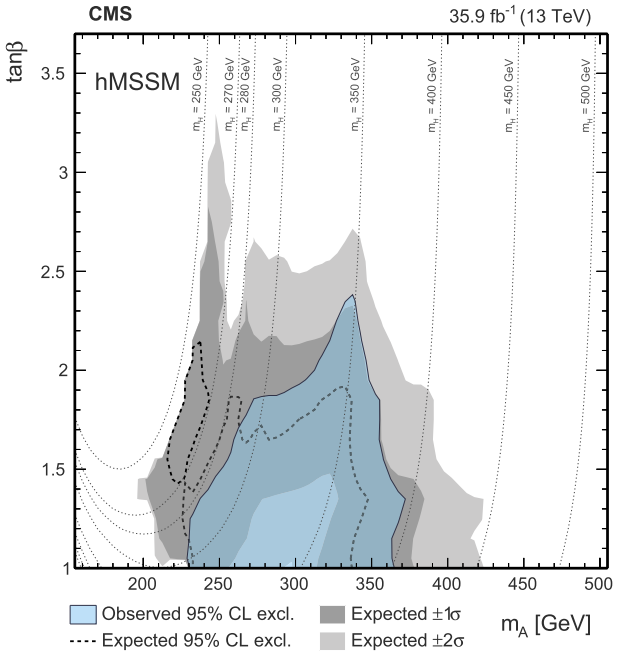

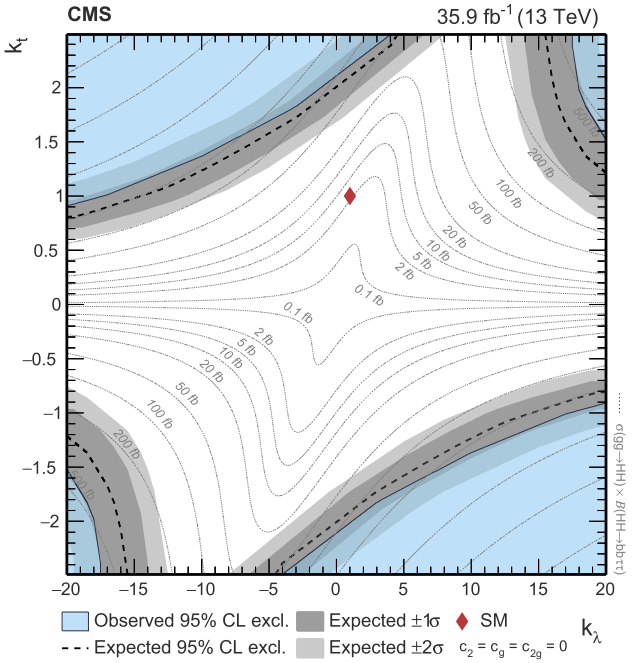

Fig. 5. (upper) Observed and expected 95% CL upper limits on cross section times branching fraction as a function of the mass of the resonance m_S under the hypothesis that its intrinsic width is negligible with respect to the experimental resolution. The inner (green) band and the outer (yellow) band indicate the regions containing 68 and 95%, respectively, of the distribution of limits expected under the background-only hypothesis. The red line denotes the expectation for the production of a radion, a spin-0 state predicted in WED models, for the parameters $\Lambda_R = 3$ TeV (mass scale) and kl = 35 (size of the extra dimension), assuming the absence of mixing with the Higgs boson. (lower) Interpretation of the exclusion limit in the context of the hMSSM model, parametrized as a function of the $\tan\beta$ and m_A parameters. In this model, the CP-even lighter scalar is assumed to be the observed 125 GeV Higgs boson and is denoted as h, while the CP-even heavier scalar is denoted as H and the CP-odd scalar is denoted as A. The dotted lines indicate trajectories in the plane corresponding to equal values of the mass of the CP-even heavier scalar of the model, m_H. (For interpretation of the references to colour in this figure legend, the reader is referred to the web version of this article.)

Fig. 6. (upper) Observed and expected 95% CL upper limits on cross section times branching fraction as a function of k_λ/k_t. The inner (green) band and the outer (yellow) band indicate the regions containing 68 and 95%, respectively, of the distribution of limits expected under the background-only hypothesis. The two red bands show the theoretical cross section expectations and the corresponding uncertainties for $k_t = 1$ and $k_t = 2$. (lower) Test of k_λ and k_t anomalous couplings. The blue region denotes the parameters excluded by the data at 95% CL, while the dashed black line and the grey regions denote the expected exclusions and the 1σ and 2σ bands. The dotted lines indicate trajectories in the plane with equal values of cross section times branching fraction that are displayed in the associated labels. The diamond-shaped symbol denotes the couplings predicted by the SM. The theory predictions and the expected and observed limits are symmetric through a $(k_\lambda, k_t) \leftrightarrow (-k_\lambda, -k_t)$ transformation. In both figures, the couplings that are not explicitly tested are assumed to correspond to the SM prediction. (For interpretation of the references to colour in this figure legend, the reader is referred to the web version of this article.)

cross section as a function of anomalous couplings of the Higgs boson. Upper limits at 95% CL on the HH cross section are obtained as a function of $k_\lambda = \lambda_{HHH}/\lambda_{HHH}^{SM}$ and $k_t = y_t/y_t^{SM}$. The observed 95% CL upper limit corresponds to approximately 30 times the theoretical prediction for the SM cross section, and the expected limit is about 25 times the SM prediction. This is the highest sensitivity achieved so far for SM HH production at the LHC.

Acknowledgments

We congratulate our colleagues in the CERN accelerator departments for the excellent performance of the LHC and thank the technical and administrative staffs at CERN and at other CMS institutes for their contributions to the success of the CMS effort. In addition, we gratefully acknowledge the computing centres and personnel of the Worldwide LHC Computing Grid for delivering so

effectively the computing infrastructure essential to our analyses. Finally, we acknowledge the enduring support for the construction and operation of the LHC and the CMS detector provided by the following funding agencies: BMWFW and FWF (Austria); FNRS and FWO (Belgium); CNPq, CAPES, FAPERJ, and FAPESP (Brazil); MES (Bulgaria); CERN; CAS, MOST, and NSFC (China); COLCIENCIAS (Colombia); MSES and CSF (Croatia); RPF (Cyprus); SENESCYT (Ecuador); MoER, ERC IUT, and ERDF (Estonia); Academy of Finland, MEC, and HIP (Finland); CEA and CNRS/IN2P3 (France); BMBF, DFG, and HGF (Germany); GSRT (Greece); OTKA and NIH (Hungary); DAE and DST (India); IPM (Iran); SFI (Ireland); INFN (Italy); MSIP and NRF (Republic of Korea); LAS (Lithuania); MOE and UM (Malaysia); BUAP, CINVESTAV, CONACYT, LNS, SEP, and UASLP-FAI (Mexico); MBIE (New Zealand); PAEC (Pakistan); MSHE and NSC (Poland); FCT (Portugal); JINR (Dubna); MON, RosAtom, RAS, RFBR and RAEP (Russia); MESTD (Serbia); SEIDI, CPAN, PCTI and FEDER (Spain); Swiss Funding Agencies (Switzerland); MST (Taipei); ThEPCenter, IPST, STAR, and NSTDA (Thailand); TUBITAK and TAEK (Turkey); NASU and SFFR (Ukraine); STFC (United Kingdom); DOE and NSF (USA).

Individuals have received support from the Marie-Curie programme and the European Research Council and Horizon 2020 Grant, contract No. 675440 (European Union); the Leventis Foundation; the Alfred P. Sloan Foundation; the Alexander von Humboldt Foundation; the Belgian Federal Science Policy Office; the Fonds pour la Formation à la Recherche dans l'Industrie et dans l'Agriculture (FRIA-Belgium); the Agentschap voor Innovatie door Wetenschap en Technologie (IWT-Belgium); the Ministry of Education, Youth and Sports (MEYS) of the Czech Republic; the Council of Science and Industrial Research, India; the HOMING PLUS programme of the Foundation for Polish Science, cofinanced from European Union, Regional Development Fund, the Mobility Plus programme of the Ministry of Science and Higher Education, the National Science Center (Poland), contracts Harmonia 2014/14/M/ST2/00428, Opus 2014/13/B/ST2/02543, 2014/15/B/ST2/03998, and 2015/19/B/ST2/02861, Sonata-bis 2012/07/E/ST2/01406; the National Priorities Research Program by Qatar National Research Fund; the Programa Clarín-COFUND del Principado de Asturias; the Thalis and Aristeia programmes cofinanced by EU-ESF and the Greek NSRF; the Rachadapisek Sompot Fund for Postdoctoral Fellowship, Chulalongkorn University and the Chulalongkorn Academic into Its 2nd Century Project Advancement Project (Thailand); and the Welch Foundation, contract C-1845.

References

[1] ATLAS Collaboration, Observation of a new particle in the search for the Standard Model Higgs boson with the ATLAS detector at the LHC, Phys. Lett. B 716 (2012) 1, https://doi.org/10.1016/j.physletb.2012.08.020, arXiv:1207.7214.

[2] CMS Collaboration, Observation of a new boson at a mass of 125 GeV with the CMS experiment at the LHC, Phys. Lett. B 716 (2012) 30, https://doi.org/10.1016/j.physletb.2012.08.021, arXiv:1207.7235.

[3] CMS Collaboration, Observation of a new boson with mass near 125 GeV in pp collisions at $\sqrt{s} = 7$ and 8 TeV, J. High Energy Phys. 06 (2013) 081, https://doi.org/10.1007/JHEP06(2013)081, arXiv:1303.4571.

[4] ATLAS and CMS Collaborations, Combined measurement of the Higgs boson mass in pp collisions at $\sqrt{s} = 7$ and 8 TeV with the ATLAS and CMS experiments, Phys. Rev. Lett. 114 (2015) 191803, https://doi.org/10.1103/PhysRevLett.114.191803, arXiv:1503.07589.

[5] ATLAS and CMS Collaborations, Measurements of the Higgs boson production and decay rates and constraints on its couplings from a combined ATLAS and CMS analysis of the LHC pp collision data at $\sqrt{s} = 7$ and 8 TeV, J. High Energy Phys. 08 (2016) 045, https://doi.org/10.1007/JHEP08(2016)045, arXiv:1606.02266.

[6] J. Baglio, A. Djouadi, R. Gröber, M.M. Mühlleitner, J. Quevillon, M. Spira, The measurement of the Higgs self-coupling at the LHC: theoretical status, J. High Energy Phys. 04 (2013) 151, https://doi.org/10.1007/JHEP04(2013)151, arXiv:1212.5581.

[7] D. de Florian, et al., Handbook of LHC Higgs cross sections: 4. Deciphering the nature of the Higgs sector, CERN Report CERN-2017-002-M, 2016, https://doi.org/10.23731/CYRM-2017-002, arXiv:1610.07922.

[8] S. Borowka, N. Greiner, G. Heinrich, S. Jones, M. Kerner, J. Schlenk, U. Schubert, T. Zirke, Higgs boson pair production in gluon fusion at next-to-leading order with full top-quark mass dependence, Phys. Rev. Lett. 117 (2016) 012001, https://doi.org/10.1103/PhysRevLett.117.012001, arXiv:1604.06447, Erratum: https://doi.org/10.1103/PhysRevLett.117.079901.

[9] S. Borowka, N. Greiner, G. Heinrich, S.P. Jones, M. Kerner, J. Schlenk, T. Zirke, Full top quark mass dependence in Higgs boson pair production at NLO, J. High Energy Phys. 10 (2016) 107, https://doi.org/10.1007/JHEP10(2016)107, arXiv:1608.04798.

[10] D. de Florian, J. Mazzitelli, Higgs pair production at next-to-next-to-leading logarithmic accuracy at the LHC, J. High Energy Phys. 09 (2015) 053, https://doi.org/10.1007/JHEP09(2015)053, arXiv:1505.07122.

[11] G. Degrassi, P.P. Giardino, R. Grober, On the two-loop virtual QCD corrections to Higgs boson pair production in the Standard Model, Eur. Phys. J. C 76 (2016) 411, https://doi.org/10.1140/epjc/s10052-016-4256-9, arXiv:1603.00385.

[12] T. Binoth, J.J. van der Bij, Influence of strongly coupled, hidden scalars on Higgs signals, Z. Phys. C 75 (1997) 17, https://doi.org/10.1007/s002880050442, arXiv:hep-ph/9608245.

[13] R.M. Schabinger, J.D. Wells, Minimal spontaneously broken hidden sector and its impact on Higgs boson physics at the CERN Large Hadron Collider, Phys. Rev. D 72 (2005) 093007, https://doi.org/10.1103/PhysRevD.72.093007, arXiv:hep-ph/0509209.

[14] B. Patt, F. Wilczek, Higgs-field portal into hidden sectors, arXiv:hep-ph/0605188, 2006.

[15] G.C. Branco, P.M. Ferreira, L. Lavoura, M.N. Rebelo, M. Sher, J.P. Silva, Theory and phenomenology of two-Higgs-doublet models, Phys. Rep. 516 (2012) 1, https://doi.org/10.1016/j.physrep.2012.02.002, arXiv:1106.0034.

[16] P. Fayet, Supergauge invariant extension of the Higgs mechanism and a model for the electron and its neutrino, Nucl. Phys. B 90 (1975) 104, https://doi.org/10.1016/0550-3213(75)90636-7.

[17] P. Fayet, Spontaneously broken supersymmetric theories of weak, electromagnetic and strong interactions, Phys. Lett. B 69 (1977) 489, https://doi.org/10.1016/0370-2693(77)90852-8.

[18] K. Agashe, H. Davoudiasl, G. Perez, A. Soni, Warped gravitons at the CERN LHC and beyond, Phys. Rev. D 76 (2007) 036006, https://doi.org/10.1103/PhysRevD.76.036006, arXiv:hep-ph/0701186.

[19] A.L. Fitzpatrick, J. Kaplan, L. Randall, L.-T. Wang, Searching for the Kaluza–Klein graviton in bulk RS models, J. High Energy Phys. 09 (2007) 013, https://doi.org/10.1088/1126-6708/2007/09/013, arXiv:hep-ph/0701150.

[20] F. Goertz, A. Papaefstathiou, L.L. Yang, J. Zurita, Higgs boson pair production in the D=6 extension of the SM, J. High Energy Phys. 04 (2015) 167, https://doi.org/10.1007/JHEP04(2015)167, arXiv:1410.3471.

[21] A. Carvalho, M. Dall'Osso, T. Dorigo, F. Goertz, C.A. Gottardo, M. Tosi, Higgs pair production: choosing benchmarks with cluster analysis, J. High Energy Phys. 04 (2016) 126, https://doi.org/10.1007/JHEP04(2016)126, arXiv:1507.02245.

[22] ATLAS Collaboration, Searches for Higgs boson pair production in the $hh \to bb\tau\tau$, $\gamma\gamma WW^*$, $\gamma\gamma bb$, $bbbb$ channels with the ATLAS detector, Phys. Rev. D 92 (2015) 092004, https://doi.org/10.1103/PhysRevD.92.092004, arXiv:1509.04670.

[23] ATLAS Collaboration, Search for pair production of Higgs bosons in the $b\bar{b}b\bar{b}$ final state using proton–proton collisions at $\sqrt{s} = 13$ TeV with the ATLAS detector, Phys. Rev. D 94 (2016) 052002, https://doi.org/10.1103/PhysRevD.94.052002, arXiv:1606.04782.

[24] CMS Collaboration, Search for two Higgs bosons in final states containing two photons and two bottom quarks in proton–proton collisions at 8 TeV, Phys. Rev. D 94 (2016) 052012, https://doi.org/10.1103/PhysRevD.94.052012, arXiv:1603.06896.

[25] CMS Collaboration, Search for resonant pair production of Higgs bosons decaying to two bottom quark–antiquark pairs in proton–proton collisions at 8 TeV, Phys. Lett. B 749 (2015) 560, https://doi.org/10.1016/j.physletb.2015.08.047, arXiv:1503.04114.

[26] CMS Collaboration, A search for Higgs boson pair production in the $bb\tau\tau$ final state in proton-proton collisions at $\sqrt{(s)} = 8$ TeV, Phys. Rev. D 96 (2017) 072004, http://dx.doi.org/10.1103/PhysRevD.96.072004, arXiv:1707.00350.

[27] CMS Collaboration, The CMS trigger system, J. Instrum. 12 (2017) P01020, https://doi.org/10.1088/1748-0221/12/01/P01020, arXiv:1609.02366.

[28] CMS Collaboration, The CMS experiment at the CERN LHC, J. Instrum. 3 (2008) S08004, https://doi.org/10.1088/1748-0221/3/08/S08004.

[29] J. Alwall, R. Frederix, S. Frixione, V. Hirschi, F. Maltoni, O. Mattelaer, H.-S. Shao, T. Stelzer, P. Torielli, M. Zaro, The automated computation of tree-level and next-to-leading order differential cross sections, and their matching to parton shower simulations, J. High Energy Phys. 07 (2014) 079, https://doi.org/10.1007/JHEP07(2014)079, arXiv:1405.0301.

[30] A. Carvalho, M. Dall'Osso, P. De Castro Manzano, T. Dorigo, F. Goertz, M. Gouzevich, M. Tosi, Analytical parametrization and shape classification of anomalous HH production in the EFT approach, 2016, http://cds.cern.ch/record/2209874, arXiv:1608.06578.

[31] J. Alwall, et al., Comparative study of various algorithms for the merging of parton showers and matrix elements in hadronic collisions, Eur. Phys. J. C 53 (2008) 473, https://doi.org/10.1140/epjc/s10052-007-0490-5, arXiv:0706.2569.
[32] E. Re, Single-top Wt-channel production matched with parton showers using the POWHEG method, Eur. Phys. J. C 71 (2011) 1547, https://doi.org/10.1140/epjc/s10052-011-1547-z, arXiv:1009.2450.
[33] J.M. Campbell, R.K. Ellis, P. Nason, E. Re, Top-pair production and decay at NLO matched with parton showers, J. High Energy Phys. 04 (2015) 114, https://doi.org/10.1007/JHEP04(2015)114, arXiv:1412.1828.
[34] R.D. Ball, et al., NNPDF, Parton distributions for the LHC Run II, J. High Energy Phys. 04 (2015) 040, https://doi.org/10.1007/JHEP04(2015)040, arXiv:1410.8849.
[35] T. Sjöstrand, S. Ask, J.R. Christiansen, R. Corke, N. Desai, P. Ilten, S. Mrenna, S. Prestel, C.O. Rasmussen, P.Z. Skands, An introduction to PYTHIA 8.2, Comput. Phys. Commun. 191 (2015) 159, https://doi.org/10.1016/j.cpc.2015.01.024, arXiv:1410.3012.
[36] CMS Collaboration, Event generator tunes obtained from underlying event and multiparton scattering measurements, Eur. Phys. J. C 76 (2016) 155, https://doi.org/10.1140/epjc/s10052-016-3988-x, arXiv:1512.00815.
[37] M. Czakon, A. Mitov, Top++: a program for the calculation of the top-pair cross-section at hadron colliders, Comput. Phys. Commun. 185 (2014) 2930, https://doi.org/10.1016/j.cpc.2014.06.021, arXiv:1112.5675.
[38] Y. Li, F. Petriello, Combining QCD and electroweak corrections to dilepton production in FEWZ, Phys. Rev. D 86 (2012) 094034, https://doi.org/10.1103/PhysRevD.86.094034, arXiv:1208.5967.
[39] N. Kidonakis, Top quark production, in: Proceedings, Helmholtz International Summer School on Physics of Heavy Quarks and Hadrons, HQ 2013, JINR, Dubna, Russia, 2014, p. 139, arXiv:1311.0283.
[40] J.M. Campbell, R.K. Ellis, C. Williams, Vector boson pair production at the LHC, J. High Energy Phys. 07 (2011) 018, https://doi.org/10.1007/JHEP07(2011)018, arXiv:1105.0020.
[41] O. Brein, R.V. Harlander, T.J.E. Zirke, vh@nnlo – Higgs Strahlung at hadron colliders, Comput. Phys. Commun. 184 (2013) 998, https://doi.org/10.1016/j.cpc.2012.11.002, arXiv:1210.5347.
[42] R.V. Harlander, S. Liebler, T. Zirke, Higgs Strahlung at the Large Hadron Collider in the 2-Higgs-doublet model, J. High Energy Phys. 02 (2014) 023, https://doi.org/10.1007/JHEP02(2014)023, arXiv:1307.8122.
[43] O. Brein, A. Djouadi, R. Harlander, NNLO QCD corrections to the Higgs-strahlung processes at hadron colliders, Phys. Lett. B 579 (2004) 149, https://doi.org/10.1016/j.physletb.2003.10.112, arXiv:hep-ph/0307206.
[44] L. Altenkamp, S. Dittmaier, R.V. Harlander, H. Rzehak, T.J.E. Zirke, Gluon-induced Higgs-strahlung at next-to-leading order QCD, J. High Energy Phys. 02 (2013) 078, https://doi.org/10.1007/JHEP02(2013)078, arXiv:1211.5015.
[45] CMS Collaboration, Particle-flow reconstruction and global event description with the CMS detector, J. Instrum. 12 (2017) P10003, https://doi.org/10.1088/1748-0221/12/10/P10003, arXiv:1706.04965.
[46] M. Cacciari, G.P. Salam, G. Soyez, The anti-k_t jet clustering algorithm, J. High Energy Phys. 04 (2008) 063, https://doi.org/10.1088/1126-6708/2008/04/063, arXiv:0802.1189.
[47] M. Cacciari, G.P. Salam, G. Soyez, FastJet user manual, Eur. Phys. J. C 72 (2012) 1896, https://doi.org/10.1140/epjc/s10052-012-1896-2, arXiv:1111.6097.
[48] J.M. Butterworth, A.R. Davison, M. Rubin, G.P. Salam, Jet substructure as a new Higgs-search channel at the Large Hadron Collider, Phys. Rev. Lett. 100 (2008) 242001, https://doi.org/10.1103/PhysRevLett.100.242001, arXiv:0802.2470.
[49] A.J. Larkoski, S. Marzani, G. Soyez, J. Thaler, Soft drop, J. High Energy Phys. 05 (2014) 146, https://doi.org/10.1007/JHEP05(2014)146, arXiv:1402.2657.
[50] CMS Collaboration, Determination of jet energy calibration and transverse momentum resolution in CMS, J. Instrum. 6 (2011) P11002, https://doi.org/10.1088/1748-0221/6/11/P11002, arXiv:1107.4277.
[51] CMS Collaboration, Performance of Missing Energy Reconstruction in 13 TeV pp Collision Data Using the CMS Detector, CMS Physics Analysis Summary CMS-PAS-JME-16-004, CERN, 2016, https://cds.cern.ch/record/2205284.
[52] CMS Collaboration, Reconstruction and identification of τ lepton decays to hadrons and ν_τ at CMS, J. Instrum. 11 (2016) P01019, https://doi.org/10.1088/1748-0221/11/01/P01019, arXiv:1510.07488.
[53] CMS Collaboration, Performance of Reconstruction and Identification of Tau Leptons in Their Decays to Hadrons and Tau Neutrino in LHC Run-2, CMS Physics Analysis Summary CMS-PAS-TAU-16-002, CERN, 2016, http://cds.cern.ch/record/2196972.
[54] CMS Collaboration, Performance of electron reconstruction and selection with the CMS detector in proton–proton collisions at $\sqrt{s} = 8$ TeV, J. Instrum. 10 (2015) P06005, https://doi.org/10.1088/1748-0221/10/06/P06005, arXiv:1502.02701.
[55] CMS Collaboration, Performance of CMS muon reconstruction in pp collision events at $\sqrt{s} = 7$ TeV, J. Instrum. 7 (2012) P10002, https://doi.org/10.1088/1748-0221/7/10/P10002, arXiv:1206.4071.
[56] CMS Collaboration, Identification of b-quark jets with the CMS experiment, J. Instrum. 8 (2013) P04013, https://doi.org/10.1088/1748-0221/8/04/P04013, arXiv:1211.4462.
[57] CMS Collaboration, Identification of b Quark Jets at the CMS Experiment in the LHC Run 2, CMS Physics Analysis Summary CMS-PAS-BTV-15-001, CERN, 2016, https://cds.cern.ch/record/2138504.
[58] L. Bianchini, J. Conway, E.K. Friis, C. Veelken, Reconstruction of the Higgs mass in $H \to \tau\tau$ events by dynamical likelihood techniques, in: Proceedings, 20th International Conference on Computing in High Energy and Nuclear Physics, CHEP 2013, Amsterdam, the Netherlands, 2014, p. 022035, J. Phys. Conf. Ser. 513 (2014) 022035.
[59] H. Voss, A. Höcker, J. Stelzer, F. Tegenfeldt, TMVA, the toolkit for multivariate data analysis with ROOT, in: XIth International Workshop on Advanced Computing and Analysis Techniques in Physics Research, ACAT, 2007, p. 40, http://pos.sissa.it/archive/conferences/050/040/ACAT_040.pdf, arXiv:physics/0703039.
[60] J.H. Friedman, Greedy function approximation: a gradient boosting machine, Ann. Stat. 29 (2001) 1189, https://doi.org/10.1214/aos/1013203451.
[61] CMS Collaboration, Searches for a heavy scalar boson H decaying to a pair of 125 GeV Higgs bosons hh or for a heavy pseudoscalar boson A decaying to Zh, in the final states with $h \to \tau\tau$, Phys. Lett. B 755 (2016) 217, https://doi.org/10.1016/j.physletb.2016.01.056, arXiv:1510.01181.
[62] C.G. Lester, D.J. Summers, Measuring masses of semi-invisibly decaying particles pair produced at hadron colliders, Phys. Lett. B 463 (1999) 99, https://doi.org/10.1016/S0370-2693(99)00945-4, arXiv:hep-ph/9906349.
[63] A. Barr, C. Lester, P. Stephens, A variable for measuring masses at hadron colliders when missing energy is expected; m_{T2}: the truth behind the glamour, J. Phys. G 29 (2003) 2343, https://doi.org/10.1088/0954-3899/29/10/304, arXiv:hep-ph/0304226.
[64] A.J. Barr, M.J. Dolan, C. Englert, M. Spannowsky, Di-Higgs final states augMT2ed – selecting hh events at the high luminosity LHC, Phys. Lett. B 728 (2014) 308, https://doi.org/10.1016/j.physletb.2013.12.011, arXiv:1309.6318.
[65] C.G. Lester, B. Nachman, Bisection-based asymmetric MT2 computation: a higher precision calculator than existing symmetric methods, J. High Energy Phys. 03 (2015) 100, https://doi.org/10.1007/JHEP03(2015)100, arXiv:1411.4312.
[66] CMS Collaboration, Measurements of differential production cross sections for a Z boson in association with jets in pp collisions at $\sqrt{s} = 8$ TeV, J. High Energy Phys. 04 (2017) 022, https://doi.org/10.1007/JHEP04(2017)022, arXiv:1611.03844.
[67] CMS Collaboration, CMS Luminosity Measurements for the 2016 Data Taking Period, CMS Physics Analysis Summary CMS-PAS-LUM-17-001, CERN, 2017, https://cds.cern.ch/record/2257069.
[68] CMS Collaboration, Measurement of differential cross sections for top quark pair production using the lepton+jets final state in proton–proton collisions at 13 TeV, Phys. Rev. D 95 (2017) 092001, https://doi.org/10.1103/PhysRevD.95.092001, arXiv:1610.04191.
[69] T. Junk, Confidence level computation for combining searches with small statistics, Nucl. Instrum. Methods A 434 (1999) 435, https://doi.org/10.1016/S0168-9002(99)00498-2, arXiv:hep-ex/9902006.
[70] A.L. Read, Presentation of search results: the CL_s technique, J. Phys. G 28 (2002) 2693, https://doi.org/10.1088/0954-3899/28/10/313.
[71] A. Oliveira, Gravity particles from Warped Extra Dimensions, predictions for LHC, arXiv:1404.0102, 2014.
[72] A. Djouadi, L. Maiani, G. Moreau, A. Polosa, J. Quevillon, V. Riquer, The post-Higgs MSSM scenario: habemus MSSM?, Eur. Phys. J. C 73 (2013) 2650, https://doi.org/10.1140/epjc/s10052-013-2650-0, arXiv:1307.5205.
[73] A. Djouadi, L. Maiani, A. Polosa, J. Quevillon, V. Riquer, Fully covering the MSSM Higgs sector at the LHC, J. High Energy Phys. 06 (2015) 168, https://doi.org/10.1007/JHEP06(2015)168, arXiv:1502.05653.

The CMS Collaboration

A.M. Sirunyan, A. Tumasyan

Yerevan Physics Institute, Yerevan, Armenia

W. Adam, F. Ambrogi, E. Asilar, T. Bergauer, J. Brandstetter, E. Brondolin, M. Dragicevic, J. Erö, M. Flechl, M. Friedl, R. Frühwirth [1], V.M. Ghete, J. Grossmann, J. Hrubec, M. Jeitler [1], A. König, N. Krammer, I. Krätschmer, D. Liko, T. Madlener, I. Mikulec, E. Pree, D. Rabady, N. Rad, H. Rohringer, J. Schieck [1], R. Schöfbeck, M. Spanring, D. Spitzbart, J. Strauss, W. Waltenberger, J. Wittmann, C.-E. Wulz [1], M. Zarucki

Institut für Hochenergiephysik, Wien, Austria

V. Chekhovsky, V. Mossolov, J. Suarez Gonzalez

Institute for Nuclear Problems, Minsk, Belarus

E.A. De Wolf, D. Di Croce, X. Janssen, J. Lauwers, H. Van Haevermaet, P. Van Mechelen, N. Van Remortel

Universiteit Antwerpen, Antwerpen, Belgium

S. Abu Zeid, F. Blekman, J. D'Hondt, I. De Bruyn, J. De Clercq, K. Deroover, G. Flouris, D. Lontkovskyi, S. Lowette, S. Moortgat, L. Moreels, A. Olbrechts, Q. Python, K. Skovpen, S. Tavernier, W. Van Doninck, P. Van Mulders, I. Van Parijs

Vrije Universiteit Brussel, Brussel, Belgium

H. Brun, B. Clerbaux, G. De Lentdecker, H. Delannoy, G. Fasanella, L. Favart, R. Goldouzian, A. Grebenyuk, G. Karapostoli, T. Lenzi, J. Luetic, T. Maerschalk, A. Marinov, A. Randle-conde, T. Seva, C. Vander Velde, P. Vanlaer, D. Vannerom, R. Yonamine, F. Zenoni, F. Zhang [2]

Université Libre de Bruxelles, Bruxelles, Belgium

A. Cimmino, T. Cornelis, D. Dobur, A. Fagot, M. Gul, I. Khvastunov, D. Poyraz, C. Roskas, S. Salva, M. Tytgat, W. Verbeke, N. Zaganidis

Ghent University, Ghent, Belgium

H. Bakhshiansohi, O. Bondu, S. Brochet, G. Bruno, A. Caudron, S. De Visscher, C. Delaere, M. Delcourt, B. Francois, A. Giammanco, A. Jafari, M. Komm, G. Krintiras, V. Lemaitre, A. Magitteri, A. Mertens, M. Musich, K. Piotrzkowski, L. Quertenmont, M. Vidal Marono, S. Wertz

Université Catholique de Louvain, Louvain-la-Neuve, Belgium

N. Beliy

Université de Mons, Mons, Belgium

W.L. Aldá Júnior, F.L. Alves, G.A. Alves, L. Brito, M. Correa Martins Junior, C. Hensel, A. Moraes, M.E. Pol, P. Rebello Teles

Centro Brasileiro de Pesquisas Fisicas, Rio de Janeiro, Brazil

E. Belchior Batista Das Chagas, W. Carvalho, J. Chinellato [3], A. Custódio, E.M. Da Costa, G.G. Da Silveira [4], D. De Jesus Damiao, S. Fonseca De Souza, L.M. Huertas Guativa, H. Malbouisson, M. Melo De Almeida, C. Mora Herrera, L. Mundim, H. Nogima, A. Santoro, A. Sznajder, E.J. Tonelli Manganote [3], F. Torres Da Silva De Araujo, A. Vilela Pereira

Universidade do Estado do Rio de Janeiro, Rio de Janeiro, Brazil

S. Ahuja [a], C.A. Bernardes [a], T.R. Fernandez Perez Tomei [a], E.M. Gregores [b], P.G. Mercadante [b], S.F. Novaes [a], Sandra S. Padula [a], D. Romero Abad [b], J.C. Ruiz Vargas [a]

[a] *Universidade Estadual Paulista, São Paulo, Brazil*
[b] *Universidade Federal do ABC, São Paulo, Brazil*

A. Aleksandrov, R. Hadjiiska, P. Iaydjiev, M. Misheva, M. Rodozov, M. Shopova, S. Stoykova, G. Sultanov

Institute for Nuclear Research and Nuclear Energy of Bulgaria Academy of Sciences, Bulgaria

A. Dimitrov, I. Glushkov, L. Litov, B. Pavlov, P. Petkov

University of Sofia, Sofia, Bulgaria

W. Fang [5], X. Gao [5]

Beihang University, Beijing, China

M. Ahmad, J.G. Bian, G.M. Chen, H.S. Chen, M. Chen, Y. Chen, C.H. Jiang, D. Leggat, H. Liao, Z. Liu, F. Romeo, S.M. Shaheen, A. Spiezia, J. Tao, C. Wang, Z. Wang, E. Yazgan, H. Zhang, J. Zhao

Institute of High Energy Physics, Beijing, China

Y. Ban, G. Chen, Q. Li, S. Liu, Y. Mao, S.J. Qian, D. Wang, Z. Xu

State Key Laboratory of Nuclear Physics and Technology, Peking University, Beijing, China

C. Avila, A. Cabrera, L.F. Chaparro Sierra, C. Florez, C.F. González Hernández, J.D. Ruiz Alvarez

Universidad de Los Andes, Bogota, Colombia

B. Courbon, N. Godinovic, D. Lelas, I. Puljak, P.M. Ribeiro Cipriano, T. Sculac

University of Split, Faculty of Electrical Engineering, Mechanical Engineering and Naval Architecture, Split, Croatia

Z. Antunovic, M. Kovac

University of Split, Faculty of Science, Split, Croatia

V. Brigljevic, D. Ferencek, K. Kadija, B. Mesic, A. Starodumov [6], T. Susa

Institute Rudjer Boskovic, Zagreb, Croatia

M.W. Ather, A. Attikis, G. Mavromanolakis, J. Mousa, C. Nicolaou, F. Ptochos, P.A. Razis, H. Rykaczewski

University of Cyprus, Nicosia, Cyprus

M. Finger [7], M. Finger Jr. [7]

Charles University, Prague, Czech Republic

E. Carrera Jarrin

Universidad San Francisco de Quito, Quito, Ecuador

E. El-khateeb [8], S. Elgammal [9], A. Mohamed [10]

Academy of Scientific Research and Technology of the Arab Republic of Egypt, Egyptian Network of High Energy Physics, Cairo, Egypt

R.K. Dewanjee, M. Kadastik, L. Perrini, M. Raidal, A. Tiko, C. Veelken

National Institute of Chemical Physics and Biophysics, Tallinn, Estonia

P. Eerola, J. Pekkanen, M. Voutilainen

Department of Physics, University of Helsinki, Helsinki, Finland

J. Härkönen, T. Järvinen, V. Karimäki, R. Kinnunen, T. Lampén, K. Lassila-Perini, S. Lehti, T. Lindén, P. Luukka, E. Tuominen, J. Tuominiemi, E. Tuovinen

Helsinki Institute of Physics, Helsinki, Finland

J. Talvitie, T. Tuuva

Lappeenranta University of Technology, Lappeenranta, Finland

M. Besancon, F. Couderc, M. Dejardin, D. Denegri, J.L. Faure, F. Ferri, S. Ganjour, S. Ghosh, A. Givernaud, P. Gras, G. Hamel de Monchenault, P. Jarry, I. Kucher, E. Locci, M. Machet, J. Malcles, G. Negro, J. Rander, A. Rosowsky, M.Ö. Sahin, M. Titov

IRFU, CEA, Université Paris-Saclay, Gif-sur-Yvette, France

A. Abdulsalam, C. Amendola, I. Antropov, S. Baffioni, F. Beaudette, P. Busson, L. Cadamuro, C. Charlot, R. Granier de Cassagnac, M. Jo, S. Lisniak, A. Lobanov, J. Martin Blanco, M. Nguyen, C. Ochando, G. Ortona, P. Paganini, P. Pigard, S. Regnard, R. Salerno, J.B. Sauvan, Y. Sirois, A.G. Stahl Leiton, T. Strebler, Y. Yilmaz, A. Zabi, A. Zghiche

Laboratoire Leprince-Ringuet, Ecole polytechnique, CNRS/IN2P3, Université Paris-Saclay, Palaiseau, France

J.-L. Agram [11], J. Andrea, D. Bloch, J.-M. Brom, M. Buttignol, E.C. Chabert, N. Chanon, C. Collard, E. Conte [11], X. Coubez, J.-C. Fontaine [11], D. Gelé, U. Goerlach, M. Jansová, A.-C. Le Bihan, N. Tonon, P. Van Hove

Université de Strasbourg, CNRS, IPHC UMR 7178, F-67000 Strasbourg, France

S. Gadrat

Centre de Calcul de l'Institut National de Physique Nucleaire et de Physique des Particules, CNRS/IN2P3, Villeurbanne, France

S. Beauceron, C. Bernet, G. Boudoul, R. Chierici, D. Contardo, P. Depasse, H. El Mamouni, J. Fay, L. Finco, S. Gascon, M. Gouzevitch, G. Grenier, B. Ille, F. Lagarde, I.B. Laktineh, M. Lethuillier, L. Mirabito, A.L. Pequegnot, S. Perries, A. Popov [12], V. Sordini, M. Vander Donckt, S. Viret

Université de Lyon, Université Claude Bernard Lyon 1, CNRS-IN2P3, Institut de Physique Nucléaire de Lyon, Villeurbanne, France

T. Toriashvili [13]

Georgian Technical University, Tbilisi, Georgia

Z. Tsamalaidze [7]

Tbilisi State University, Tbilisi, Georgia

C. Autermann, S. Beranek, L. Feld, M.K. Kiesel, K. Klein, M. Lipinski, M. Preuten, C. Schomakers, J. Schulz, T. Verlage

RWTH Aachen University, I. Physikalisches Institut, Aachen, Germany

A. Albert, E. Dietz-Laursonn, D. Duchardt, M. Endres, M. Erdmann, S. Erdweg, T. Esch, R. Fischer, A. Güth, M. Hamer, T. Hebbeker, C. Heidemann, K. Hoepfner, S. Knutzen, M. Merschmeyer, A. Meyer, P. Millet, S. Mukherjee, M. Olschewski, K. Padeken, T. Pook, M. Radziej, H. Reithler, M. Rieger, F. Scheuch, D. Teyssier, S. Thüer

RWTH Aachen University, III. Physikalisches Institut A, Aachen, Germany

G. Flügge, B. Kargoll, T. Kress, A. Künsken, J. Lingemann, T. Müller, A. Nehrkorn, A. Nowack, C. Pistone, O. Pooth, A. Stahl [14]

RWTH Aachen University, III. Physikalisches Institut B, Aachen, Germany

M. Aldaya Martin, T. Arndt, C. Asawatangtrakuldee, K. Beernaert, O. Behnke, U. Behrens, A. Bermúdez Martínez, A.A. Bin Anuar, K. Borras [15], V. Botta, A. Campbell, P. Connor, C. Contreras-Campana, F. Costanza, C. Diez Pardos, G. Eckerlin, D. Eckstein, T. Eichhorn, E. Eren, E. Gallo [16], J. Garay Garcia, A. Geiser, A. Gizhko, J.M. Grados Luyando, A. Grohsjean, P. Gunnellini, A. Harb, J. Hauk, M. Hempel [17], H. Jung, A. Kalogeropoulos, M. Kasemann, J. Keaveney, C. Kleinwort, I. Korol, D. Krücker, W. Lange, A. Lelek, T. Lenz, J. Leonard, K. Lipka, W. Lohmann [17], R. Mankel, I.-A. Melzer-Pellmann, A.B. Meyer, G. Mittag, J. Mnich, A. Mussgiller, E. Ntomari, D. Pitzl, R. Placakyte,

A. Raspereza, B. Roland, M. Savitskyi, P. Saxena, R. Shevchenko, S. Spannagel, N. Stefaniuk, G.P. Van Onsem, R. Walsh, Y. Wen, K. Wichmann, C. Wissing, O. Zenaiev

Deutsches Elektronen-Synchrotron, Hamburg, Germany

S. Bein, V. Blobel, M. Centis Vignali, T. Dreyer, E. Garutti, D. Gonzalez, J. Haller, A. Hinzmann, M. Hoffmann, A. Karavdina, R. Klanner, R. Kogler, N. Kovalchuk, S. Kurz, T. Lapsien, I. Marchesini, D. Marconi, M. Meyer, M. Niedziela, D. Nowatschin, F. Pantaleo [14], T. Peiffer, A. Perieanu, C. Scharf, P. Schleper, A. Schmidt, S. Schumann, J. Schwandt, J. Sonneveld, H. Stadie, G. Steinbrück, F.M. Stober, M. Stöver, H. Tholen, D. Troendle, E. Usai, L. Vanelderen, A. Vanhoefer, B. Vormwald

University of Hamburg, Hamburg, Germany

M. Akbiyik, C. Barth, S. Baur, E. Butz, R. Caspart, T. Chwalek, F. Colombo, W. De Boer, A. Dierlamm, B. Freund, R. Friese, M. Giffels, A. Gilbert, D. Haitz, F. Hartmann [14], S.M. Heindl, U. Husemann, F. Kassel [14], S. Kudella, H. Mildner, M.U. Mozer, Th. Müller, M. Plagge, G. Quast, K. Rabbertz, M. Schröder, I. Shvetsov, G. Sieber, H.J. Simonis, R. Ulrich, S. Wayand, M. Weber, T. Weiler, S. Williamson, C. Wöhrmann, R. Wolf

Institut für Experimentelle Kernphysik, Karlsruhe, Germany

G. Anagnostou, G. Daskalakis, T. Geralis, V.A. Giakoumopoulou, A. Kyriakis, D. Loukas, I. Topsis-Giotis

Institute of Nuclear and Particle Physics (INPP), NCSR Demokritos, Aghia Paraskevi, Greece

S. Kesisoglou, A. Panagiotou, N. Saoulidou

National and Kapodistrian University of Athens, Athens, Greece

I. Evangelou, C. Foudas, P. Kokkas, S. Mallios, N. Manthos, I. Papadopoulos, E. Paradas, J. Strologas, F.A. Triantis

University of Ioánnina, Ioánnina, Greece

M. Csanad, N. Filipovic, G. Pasztor

MTA-ELTE Lendület CMS Particle and Nuclear Physics Group, Eötvös Loránd University, Budapest, Hungary

G. Bencze, C. Hajdu, D. Horvath [18], Á. Hunyadi, F. Sikler, V. Veszpremi, G. Vesztergombi [19], A.J. Zsigmond

Wigner Research Centre for Physics, Budapest, Hungary

N. Beni, S. Czellar, J. Karancsi [20], A. Makovec, J. Molnar, Z. Szillasi

Institute of Nuclear Research ATOMKI, Debrecen, Hungary

M. Bartók [19], P. Raics, Z.L. Trocsanyi, B. Ujvari

Institute of Physics, University of Debrecen, Debrecen, Hungary

S. Choudhury, J.R. Komaragiri

Indian Institute of Science (IISc), Bangalore, India

S. Bahinipati [21], S. Bhowmik, P. Mal, K. Mandal, A. Nayak [22], D.K. Sahoo [21], N. Sahoo, S.K. Swain

National Institute of Science Education and Research, Bhubaneswar, India

S. Bansal, S.B. Beri, V. Bhatnagar, U. Bhawandeep, R. Chawla, N. Dhingra, A.K. Kalsi, A. Kaur, M. Kaur, R. Kumar, P. Kumari, A. Mehta, J.B. Singh, G. Walia

Panjab University, Chandigarh, India

Ashok Kumar, Aashaq Shah, A. Bhardwaj, S. Chauhan, B.C. Choudhary, R.B. Garg, S. Keshri, A. Kumar, S. Malhotra, M. Naimuddin, K. Ranjan, R. Sharma, V. Sharma

University of Delhi, Delhi, India

R. Bhardwaj, R. Bhattacharya, S. Bhattacharya, S. Dey, S. Dutt, S. Dutta, S. Ghosh, N. Majumdar, A. Modak, K. Mondal, S. Mukhopadhyay, S. Nandan, A. Purohit, A. Roy, D. Roy, S. Roy Chowdhury, S. Sarkar, M. Sharan, S. Thakur

Saha Institute of Nuclear Physics, HBNI, Kolkata, India

P.K. Behera

Indian Institute of Technology Madras, Madras, India

R. Chudasama, D. Dutta, V. Jha, V. Kumar, A.K. Mohanty [14], P.K. Netrakanti, L.M. Pant, P. Shukla, A. Topkar

Bhabha Atomic Research Centre, Mumbai, India

T. Aziz, S. Dugad, B. Mahakud, S. Mitra, G.B. Mohanty, N. Sur, B. Sutar

Tata Institute of Fundamental Research-A, Mumbai, India

S. Banerjee, S. Bhattacharya, S. Chatterjee, P. Das, M. Guchait, Sa. Jain, S. Kumar, M. Maity [23], G. Majumder, K. Mazumdar, T. Sarkar [23], N. Wickramage [24]

Tata Institute of Fundamental Research-B, Mumbai, India

S. Chauhan, S. Dube, V. Hegde, A. Kapoor, K. Kothekar, S. Pandey, A. Rane, S. Sharma

Indian Institute of Science Education and Research (IISER), Pune, India

S. Chenarani [25], E. Eskandari Tadavani, S.M. Etesami [25], M. Khakzad, M. Mohammadi Najafabadi, M. Naseri, S. Paktinat Mehdiabadi [26], F. Rezaei Hosseinabadi, B. Safarzadeh [27], M. Zeinali

Institute for Research in Fundamental Sciences (IPM), Tehran, Iran

M. Felcini, M. Grunewald

University College Dublin, Dublin, Ireland

M. Abbrescia [a,b], C. Calabria [a,b], C. Caputo [a,b], A. Colaleo [a], D. Creanza [a,c], L. Cristella [a,b], N. De Filippis [a,c], M. De Palma [a,b], F. Errico [a,b], L. Fiore [a], G. Iaselli [a,c], S. Lezki [a,b], G. Maggi [a,c], M. Maggi [a], G. Miniello [a,b], S. My [a,b], S. Nuzzo [a,b], A. Pompili [a,b], G. Pugliese [a,c], R. Radogna [a,b], A. Ranieri [a], G. Selvaggi [a,b], A. Sharma [a], L. Silvestris [a,14], R. Venditti [a], P. Verwilligen [a]

[a] *INFN Sezione di Bari, Bari, Italy*
[b] *Università di Bari, Bari, Italy*
[c] *Politecnico di Bari, Bari, Italy*

G. Abbiendi [a], C. Battilana [a,b], D. Bonacorsi [a,b], S. Braibant-Giacomelli [a,b], R. Campanini [a,b], P. Capiluppi [a,b], A. Castro [a,b], F.R. Cavallo [a], S.S. Chhibra [a], G. Codispoti [a,b], M. Cuffiani [a,b], G.M. Dallavalle [a], F. Fabbri [a], A. Fanfani [a,b], D. Fasanella [a,b], P. Giacomelli [a], C. Grandi [a], L. Guiducci [a,b], S. Marcellini [a], G. Masetti [a], A. Montanari [a], F.L. Navarria [a,b], A. Perrotta [a], A.M. Rossi [a,b], T. Rovelli [a,b], G.P. Siroli [a,b], N. Tosi [a]

[a] *INFN Sezione di Bologna, Bologna, Italy*
[b] *Università di Bologna, Bologna, Italy*

S. Albergo [a,b], S. Costa [a,b], A. Di Mattia [a], F. Giordano [a,b], R. Potenza [a,b], A. Tricomi [a,b], C. Tuve [a,b]

[a] *INFN Sezione di Catania, Catania, Italy*
[b] *Università di Catania, Catania, Italy*

G. Barbagli [a], K. Chatterjee [a,b], V. Ciulli [a,b], C. Civinini [a], R. D'Alessandro [a,b], E. Focardi [a,b], P. Lenzi [a,b], M. Meschini [a], S. Paoletti [a], L. Russo [a,28], G. Sguazzoni [a], D. Strom [a], L. Viliani [a,b,14]

[a] INFN Sezione di Firenze, Firenze, Italy
[b] Università di Firenze, Firenze, Italy

L. Benussi, S. Bianco, F. Fabbri, D. Piccolo, F. Primavera [14]

INFN Laboratori Nazionali di Frascati, Frascati, Italy

V. Calvelli [a,b], F. Ferro [a], E. Robutti [a], S. Tosi [a,b]

[a] INFN Sezione di Genova, Genova, Italy
[b] Università di Genova, Genova, Italy

L. Brianza [a,b], F. Brivio [a,b], V. Ciriolo [a,b], M.E. Dinardo [a,b], S. Fiorendi [a,b], S. Gennai [a], A. Ghezzi [a,b], P. Govoni [a,b], M. Malberti [a,b], S. Malvezzi [a], R.A. Manzoni [a,b], D. Menasce [a], L. Moroni [a], M. Paganoni [a,b], K. Pauwels [a,b], D. Pedrini [a], S. Pigazzini [a,b,29], S. Ragazzi [a,b], T. Tabarelli de Fatis [a,b]

[a] INFN Sezione di Milano-Bicocca, Milano, Italy
[b] Università di Milano-Bicocca, Milano, Italy

S. Buontempo [a], N. Cavallo [a,c], S. Di Guida [a,d,14], F. Fabozzi [a,c], F. Fienga [a,b], A.O.M. Iorio [a,b], W.A. Khan [a], L. Lista [a], S. Meola [a,d,14], P. Paolucci [a,14], C. Sciacca [a,b], F. Thyssen [a]

[a] INFN Sezione di Napoli, Napoli, Italy
[b] Università di Napoli 'Federico II', Napoli, Italy
[c] Università della Basilicata, Potenza, Italy
[d] Università G. Marconi, Roma, Italy

P. Azzi [a,14], N. Bacchetta [a], L. Benato [a,b], D. Bisello [a,b], A. Boletti [a,b], R. Carlin [a,b], A. Carvalho Antunes De Oliveira [a,b], M. Dall'Osso [a,b], P. De Castro Manzano [a], T. Dorigo [a], U. Dosselli [a], S. Fantinel [a], F. Fanzago [a], A. Gozzelino [a], S. Lacaprara [a], P. Lujan, M. Margoni [a,b], A.T. Meneguzzo [a,b], N. Pozzobon [a,b], P. Ronchese [a,b], R. Rossin [a,b], F. Simonetto [a,b], E. Torassa [a], M. Zanetti [a,b], P. Zotto [a,b], G. Zumerle [a,b]

[a] INFN Sezione di Padova, Padova, Italy
[b] Università di Padova, Padova, Italy
[c] Università di Trento, Trento, Italy

A. Braghieri [a], F. Fallavollita [a,b], A. Magnani [a,b], P. Montagna [a,b], S.P. Ratti [a,b], V. Re [a], M. Ressegotti, C. Riccardi [a,b], P. Salvini [a], I. Vai [a,b], P. Vitulo [a,b]

[a] INFN Sezione di Pavia, Pavia, Italy
[b] Università di Pavia, Pavia, Italy

L. Alunni Solestizi [a,b], M. Biasini [a,b], G.M. Bilei [a], C. Cecchi [a,b], D. Ciangottini [a,b], L. Fanò [a,b], P. Lariccia [a,b], R. Leonardi [a,b], E. Manoni [a], G. Mantovani [a,b], V. Mariani [a,b], M. Menichelli [a], A. Rossi [a,b], A. Santocchia [a,b], D. Spiga [a]

[a] INFN Sezione di Perugia, Perugia, Italy
[b] Università di Perugia, Perugia, Italy

K. Androsov [a], P. Azzurri [a,14], G. Bagliesi [a], J. Bernardini [a], T. Boccali [a], L. Borrello, R. Castaldi [a], M.A. Ciocci [a,b], R. Dell'Orso [a], G. Fedi [a], L. Giannini [a,c], A. Giassi [a], M.T. Grippo [a,28], F. Ligabue [a,c], T. Lomtadze [a], E. Manca [a,c], G. Mandorli [a,c], L. Martini [a,b], A. Messineo [a,b], F. Palla [a], A. Rizzi [a,b], A. Savoy-Navarro [a,30], P. Spagnolo [a], R. Tenchini [a], G. Tonelli [a,b], A. Venturi [a], P.G. Verdini [a]

[a] INFN Sezione di Pisa, Pisa, Italy
[b] Università di Pisa, Pisa, Italy
[c] Scuola Normale Superiore di Pisa, Pisa, Italy

L. Barone [a,b], F. Cavallari [a], M. Cipriani [a,b], D. Del Re [a,b,14], M. Diemoz [a], S. Gelli [a,b], E. Longo [a,b], F. Margaroli [a,b], B. Marzocchi [a,b], P. Meridiani [a], G. Organtini [a,b], R. Paramatti [a,b], F. Preiato [a,b], S. Rahatlou [a,b], C. Rovelli [a], F. Santanastasio [a,b]

[a] INFN Sezione di Roma, Rome, Italy
[b] Sapienza Università di Roma, Rome, Italy

N. Amapane [a,b], R. Arcidiacono [a,c], S. Argiro [a,b], M. Arneodo [a,c], N. Bartosik [a], R. Bellan [a,b], C. Biino [a], N. Cartiglia [a], F. Cenna [a,b], M. Costa [a,b], R. Covarelli [a,b], A. Degano [a,b], N. Demaria [a], B. Kiani [a,b], C. Mariotti [a], S. Maselli [a], E. Migliore [a,b], V. Monaco [a,b], E. Monteil [a,b], M. Monteno [a], M.M. Obertino [a,b], L. Pacher [a,b], N. Pastrone [a], M. Pelliccioni [a], G.L. Pinna Angioni [a,b], F. Ravera [a,b], A. Romero [a,b], M. Ruspa [a,c], R. Sacchi [a,b], K. Shchelina [a,b], V. Sola [a], A. Solano [a,b], A. Staiano [a], P. Traczyk [a,b]

[a] INFN Sezione di Torino, Torino, Italy
[b] Università di Torino, Torino, Italy
[c] Università del Piemonte Orientale, Novara, Italy

S. Belforte [a], M. Casarsa [a], F. Cossutti [a], G. Della Ricca [a,b], A. Zanetti [a]

[a] INFN Sezione di Trieste, Trieste, Italy
[b] Università di Trieste, Trieste, Italy

D.H. Kim, G.N. Kim, M.S. Kim, J. Lee, S. Lee, S.W. Lee, C.S. Moon, Y.D. Oh, S. Sekmen, D.C. Son, Y.C. Yang

Kyungpook National University, Daegu, Republic of Korea

A. Lee

Chonbuk National University, Jeonju, Republic of Korea

H. Kim, D.H. Moon, G. Oh

Chonnam National University, Institute for Universe and Elementary Particles, Kwangju, Republic of Korea

J.A. Brochero Cifuentes, J. Goh, T.J. Kim

Hanyang University, Seoul, Republic of Korea

S. Cho, S. Choi, Y. Go, D. Gyun, S. Ha, B. Hong, Y. Jo, Y. Kim, K. Lee, K.S. Lee, S. Lee, J. Lim, S.K. Park, Y. Roh

Korea University, Seoul, Republic of Korea

J. Almond, J. Kim, J.S. Kim, H. Lee, K. Lee, K. Nam, S.B. Oh, B.C. Radburn-Smith, S.h. Seo, U.K. Yang, H.D. Yoo, G.B. Yu

Seoul National University, Seoul, Republic of Korea

M. Choi, H. Kim, J.H. Kim, J.S.H. Lee, I.C. Park, G. Ryu

University of Seoul, Seoul, Republic of Korea

Y. Choi, C. Hwang, J. Lee, I. Yu

Sungkyunkwan University, Suwon, Republic of Korea

V. Dudenas, A. Juodagalvis, J. Vaitkus

Vilnius University, Vilnius, Lithuania

I. Ahmed, Z.A. Ibrahim, M.A.B. Md Ali [31], F. Mohamad Idris [32], W.A.T. Wan Abdullah, M.N. Yusli, Z. Zolkapli

National Centre for Particle Physics, Universiti Malaya, Kuala Lumpur, Malaysia

M.C. Duran-Osuna, H. Castilla-Valdez, E. De La Cruz-Burelo, I. Heredia-De La Cruz [33], R. Lopez-Fernandez, J. Mejia Guisao, R.I. Rabadán-Trejo, G. Ramirez-Sanchez, R. Reyes-Almanza, A. Sanchez-Hernandez

Centro de Investigacion y de Estudios Avanzados del IPN, Mexico City, Mexico

S. Carrillo Moreno, C. Oropeza Barrera, F. Vazquez Valencia

Universidad Iberoamericana, Mexico City, Mexico

I. Pedraza, H.A. Salazar Ibarguen, C. Uribe Estrada

Benemerita Universidad Autonoma de Puebla, Puebla, Mexico

A. Morelos Pineda

Universidad Autónoma de San Luis Potosí, San Luis Potosí, Mexico

D. Krofcheck

University of Auckland, Auckland, New Zealand

P.H. Butler

University of Canterbury, Christchurch, New Zealand

A. Ahmad, M. Ahmad, Q. Hassan, H.R. Hoorani, A. Saddique, M.A. Shah, M. Shoaib, M. Waqas

National Centre for Physics, Quaid-I-Azam University, Islamabad, Pakistan

H. Bialkowska, M. Bluj, B. Boimska, T. Frueboes, M. Górski, M. Kazana, K. Nawrocki, K. Romanowska-Rybinska, M. Szleper, P. Zalewski

National Centre for Nuclear Research, Swierk, Poland

K. Bunkowski, A. Byszuk [34], K. Doroba, A. Kalinowski, M. Konecki, J. Krolikowski, M. Misiura, M. Olszewski, A. Pyskir, M. Walczak

Institute of Experimental Physics, Faculty of Physics, University of Warsaw, Warsaw, Poland

P. Bargassa, C. Beirão Da Cruz E Silva, B. Calpas, A. Di Francesco, P. Faccioli, M. Gallinaro, J. Hollar, N. Leonardo, L. Lloret Iglesias, M.V. Nemallapudi, J. Seixas, O. Toldaiev, D. Vadruccio, J. Varela

Laboratório de Instrumentação e Física Experimental de Partículas, Lisboa, Portugal

S. Afanasiev, P. Bunin, M. Gavrilenko, I. Golutvin, I. Gorbunov, A. Kamenev, V. Karjavin, A. Lanev, A. Malakhov, V. Matveev [35,36], V. Palichik, V. Perelygin, S. Shmatov, S. Shulha, N. Skatchkov, V. Smirnov, N. Voytishin, A. Zarubin

Joint Institute for Nuclear Research, Dubna, Russia

Y. Ivanov, V. Kim [37], E. Kuznetsova [38], P. Levchenko, V. Murzin, V. Oreshkin, I. Smirnov, V. Sulimov, L. Uvarov, S. Vavilov, A. Vorobyev

Petersburg Nuclear Physics Institute, Gatchina (St. Petersburg), Russia

Yu. Andreev, A. Dermenev, S. Gninenko, N. Golubev, A. Karneyeu, M. Kirsanov, N. Krasnikov, A. Pashenkov, D. Tlisov, A. Toropin

Institute for Nuclear Research, Moscow, Russia

V. Epshteyn, V. Gavrilov, N. Lychkovskaya, V. Popov, I. Pozdnyakov, G. Safronov, A. Spiridonov, A. Stepennov, M. Toms, E. Vlasov, A. Zhokin

Institute for Theoretical and Experimental Physics, Moscow, Russia

T. Aushev, A. Bylinkin [36]

Moscow Institute of Physics and Technology, Moscow, Russia

R. Chistov [39], M. Danilov [39], P. Parygin, D. Philippov, S. Polikarpov, E. Tarkovskii

National Research Nuclear University 'Moscow Engineering Physics Institute' (MEPhI), Moscow, Russia

V. Andreev, M. Azarkin [36], I. Dremin [36], M. Kirakosyan [36], A. Terkulov

P.N. Lebedev Physical Institute, Moscow, Russia

A. Baskakov, A. Belyaev, E. Boos, V. Bunichev, M. Dubinin [40], L. Dudko, A. Ershov, A. Gribushin, V. Klyukhin, O. Kodolova, I. Lokhtin, I. Miagkov, S. Obraztsov, S. Petrushanko, V. Savrin

Skobeltsyn Institute of Nuclear Physics, Lomonosov Moscow State University, Moscow, Russia

V. Blinov [41], Y. Skovpen [41], D. Shtol [41]

Novosibirsk State University (NSU), Novosibirsk, Russia

I. Azhgirey, I. Bayshev, S. Bitioukov, D. Elumakhov, V. Kachanov, A. Kalinin, D. Konstantinov, V. Krychkine, V. Petrov, R. Ryutin, A. Sobol, S. Troshin, N. Tyurin, A. Uzunian, A. Volkov

State Research Center of Russian Federation, Institute for High Energy Physics, Protvino, Russia

P. Adzic [42], P. Cirkovic, D. Devetak, M. Dordevic, J. Milosevic, V. Rekovic

University of Belgrade, Faculty of Physics and Vinca Institute of Nuclear Sciences, Belgrade, Serbia

J. Alcaraz Maestre, M. Barrio Luna, M. Cerrada, N. Colino, B. De La Cruz, A. Delgado Peris, A. Escalante Del Valle, C. Fernandez Bedoya, J.P. Fernández Ramos, J. Flix, M.C. Fouz, P. Garcia-Abia, O. Gonzalez Lopez, S. Goy Lopez, J.M. Hernandez, M.I. Josa, A. Pérez-Calero Yzquierdo, J. Puerta Pelayo, A. Quintario Olmeda, I. Redondo, L. Romero, M.S. Soares, A. Álvarez Fernández

Centro de Investigaciones Energéticas Medioambientales y Tecnológicas (CIEMAT), Madrid, Spain

J.F. de Trocóniz, M. Missiroli, D. Moran

Universidad Autónoma de Madrid, Madrid, Spain

J. Cuevas, C. Erice, J. Fernandez Menendez, I. Gonzalez Caballero, J.R. González Fernández, E. Palencia Cortezon, S. Sanchez Cruz, I. Suárez Andrés, P. Vischia, J.M. Vizan Garcia

Universidad de Oviedo, Oviedo, Spain

I.J. Cabrillo, A. Calderon, B. Chazin Quero, E. Curras, M. Fernandez, J. Garcia-Ferrero, G. Gomez, A. Lopez Virto, J. Marco, C. Martinez Rivero, P. Martinez Ruiz del Arbol, F. Matorras, J. Piedra Gomez, T. Rodrigo, A. Ruiz-Jimeno, L. Scodellaro, N. Trevisani, I. Vila, R. Vilar Cortabitarte

Instituto de Física de Cantabria (IFCA), CSIC-Universidad de Cantabria, Santander, Spain

D. Abbaneo, E. Auffray, P. Baillon, A.H. Ball, D. Barney, M. Bianco, P. Bloch, A. Bocci, C. Botta, T. Camporesi, R. Castello, M. Cepeda, G. Cerminara, E. Chapon, Y. Chen, D. d'Enterria, A. Dabrowski, V. Daponte, A. David, M. De Gruttola, A. De Roeck, E. Di Marco [43], M. Dobson, B. Dorney, T. du Pree, M. Dünser, N. Dupont, A. Elliott-Peisert, P. Everaerts, G. Franzoni, J. Fulcher, W. Funk, D. Gigi, K. Gill, F. Glege, D. Gulhan, S. Gundacker, M. Guthoff, P. Harris, J. Hegeman, V. Innocente, P. Janot, O. Karacheban [17], J. Kieseler, H. Kirschenmann, V. Knünz, A. Kornmayer [14], M.J. Kortelainen, C. Lange, P. Lecoq, C. Lourenço, M.T. Lucchini, L. Malgeri, M. Mannelli, A. Martelli, F. Meijers, J.A. Merlin, S. Mersi, E. Meschi, P. Milenovic [44], F. Moortgat, M. Mulders, H. Neugebauer, S. Orfanelli, L. Orsini, L. Pape, E. Perez, M. Peruzzi, A. Petrilli, G. Petrucciani, A. Pfeiffer, M. Pierini, A. Racz, T. Reis, G. Rolandi [45], M. Rovere, H. Sakulin, C. Schäfer, C. Schwick, M. Seidel, M. Selvaggi, A. Sharma, P. Silva, P. Sphicas [46],

J. Steggemann, M. Stoye, M. Tosi, D. Treille, A. Triossi, A. Tsirou, V. Veckalns [47], G.I. Veres [19], M. Verweij, N. Wardle, W.D. Zeuner

CERN, European Organization for Nuclear Research, Geneva, Switzerland

W. Bertl [†], L. Caminada [48], K. Deiters, W. Erdmann, R. Horisberger, Q. Ingram, H.C. Kaestli, D. Kotlinski, U. Langenegger, T. Rohe, S.A. Wiederkehr

Paul Scherrer Institut, Villigen, Switzerland

F. Bachmair, L. Bäni, P. Berger, L. Bianchini, B. Casal, G. Dissertori, M. Dittmar, M. Donegà, C. Grab, C. Heidegger, D. Hits, J. Hoss, G. Kasieczka, T. Klijnsma, W. Lustermann, B. Mangano, M. Marionneau, M.T. Meinhard, D. Meister, F. Micheli, P. Musella, F. Nessi-Tedaldi, F. Pandolfi, J. Pata, F. Pauss, G. Perrin, L. Perrozzi, M. Quittnat, M. Schönenberger, L. Shchutska, V.R. Tavolaro, K. Theofilatos, M.L. Vesterbacka Olsson, R. Wallny, A. Zagozdzinska [34], D.H. Zhu

Institute for Particle Physics, ETH Zurich, Zurich, Switzerland

T.K. Aarrestad, C. Amsler [49], M.F. Canelli, A. De Cosa, R. Del Burgo, S. Donato, C. Galloni, T. Hreus, B. Kilminster, J. Ngadiuba, D. Pinna, G. Rauco, P. Robmann, D. Salerno, C. Seitz, Y. Takahashi, A. Zucchetta

Universität Zürich, Zurich, Switzerland

V. Candelise, T.H. Doan, Sh. Jain, R. Khurana, C.M. Kuo, W. Lin, A. Pozdnyakov, S.S. Yu

National Central University, Chung-Li, Taiwan

Arun Kumar, P. Chang, Y. Chao, K.F. Chen, P.H. Chen, F. Fiori, W.-S. Hou, Y. Hsiung, Y.F. Liu, R.-S. Lu, M. Miñano Moya, E. Paganis, A. Psallidas, J.f. Tsai

National Taiwan University (NTU), Taipei, Taiwan

B. Asavapibhop, K. Kovitanggoon, G. Singh, N. Srimanobhas

Chulalongkorn University, Faculty of Science, Department of Physics, Bangkok, Thailand

A. Adiguzel [50], F. Boran, S. Cerci [51], S. Damarseckin, Z.S. Demiroglu, C. Dozen, I. Dumanoglu, S. Girgis, G. Gokbulut, Y. Guler, I. Hos [52], E.E. Kangal [53], O. Kara, A. Kayis Topaksu, U. Kiminsu, M. Oglakci, G. Onengut [54], K. Ozdemir [55], D. Sunar Cerci [51], B. Tali [51], S. Turkcapar, I.S. Zorbakir, C. Zorbilmez

Çukurova University, Physics Department, Science and Art Faculty, Adana, Turkey

B. Bilin, G. Karapinar [56], K. Ocalan [57], M. Yalvac, M. Zeyrek

Middle East Technical University, Physics Department, Ankara, Turkey

E. Gülmez, M. Kaya [58], O. Kaya [59], S. Tekten, E.A. Yetkin [60]

Bogazici University, Istanbul, Turkey

M.N. Agaras, S. Atay, A. Cakir, K. Cankocak

Istanbul Technical University, Istanbul, Turkey

B. Grynyov

Institute for Scintillation Materials of National Academy of Science of Ukraine, Kharkov, Ukraine

L. Levchuk, P. Sorokin

National Scientific Center, Kharkov Institute of Physics and Technology, Kharkov, Ukraine

R. Aggleton, F. Ball, L. Beck, J.J. Brooke, D. Burns, E. Clement, D. Cussans, O. Davignon, H. Flacher, J. Goldstein, M. Grimes, G.P. Heath, H.F. Heath, J. Jacob, L. Kreczko, C. Lucas, D.M. Newbold [61], S. Paramesvaran, A. Poll, T. Sakuma, S. Seif El Nasr-storey, D. Smith, V.J. Smith

University of Bristol, Bristol, United Kingdom

K.W. Bell, A. Belyaev [62], C. Brew, R.M. Brown, L. Calligaris, D. Cieri, D.J.A. Cockerill, J.A. Coughlan, K. Harder, S. Harper, E. Olaiya, D. Petyt, C.H. Shepherd-Themistocleous, A. Thea, I.R. Tomalin, T. Williams

Rutherford Appleton Laboratory, Didcot, United Kingdom

R. Bainbridge, S. Breeze, O. Buchmuller, A. Bundock, S. Casasso, M. Citron, D. Colling, L. Corpe, P. Dauncey, G. Davies, A. De Wit, M. Della Negra, R. Di Maria, A. Elwood, Y. Haddad, G. Hall, G. Iles, T. James, R. Lane, C. Laner, L. Lyons, A.-M. Magnan, S. Malik, L. Mastrolorenzo, T. Matsushita, J. Nash, A. Nikitenko [6], V. Palladino, M. Pesaresi, D.M. Raymond, A. Richards, A. Rose, E. Scott, C. Seez, A. Shtipliyski, S. Summers, A. Tapper, K. Uchida, M. Vazquez Acosta [63], T. Virdee [14], D. Winterbottom, J. Wright, S.C. Zenz

Imperial College, London, United Kingdom

J.E. Cole, P.R. Hobson, A. Khan, P. Kyberd, I.D. Reid, P. Symonds, L. Teodorescu, M. Turner

Brunel University, Uxbridge, United Kingdom

A. Borzou, K. Call, J. Dittmann, K. Hatakeyama, H. Liu, N. Pastika, C. Smith

Baylor University, Waco, USA

R. Bartek, A. Dominguez

Catholic University of America, Washington DC, USA

A. Buccilli, S.I. Cooper, C. Henderson, P. Rumerio, C. West

The University of Alabama, Tuscaloosa, USA

D. Arcaro, A. Avetisyan, T. Bose, D. Gastler, D. Rankin, C. Richardson, J. Rohlf, L. Sulak, D. Zou

Boston University, Boston, USA

G. Benelli, D. Cutts, A. Garabedian, J. Hakala, U. Heintz, J.M. Hogan, K.H.M. Kwok, E. Laird, G. Landsberg, Z. Mao, M. Narain, S. Piperov, S. Sagir, R. Syarif, D. Yu

Brown University, Providence, USA

R. Band, C. Brainerd, D. Burns, M. Calderon De La Barca Sanchez, M. Chertok, J. Conway, R. Conway, P.T. Cox, R. Erbacher, C. Flores, G. Funk, M. Gardner, W. Ko, R. Lander, C. Mclean, M. Mulhearn, D. Pellett, J. Pilot, S. Shalhout, M. Shi, J. Smith, M. Squires, D. Stolp, K. Tos, M. Tripathi, Z. Wang

University of California, Davis, Davis, USA

M. Bachtis, C. Bravo, R. Cousins, A. Dasgupta, A. Florent, J. Hauser, M. Ignatenko, N. Mccoll, D. Saltzberg, C. Schnaible, V. Valuev

University of California, Los Angeles, USA

E. Bouvier, K. Burt, R. Clare, J. Ellison, J.W. Gary, S.M.A. Ghiasi Shirazi, G. Hanson, J. Heilman, P. Jandir, E. Kennedy, F. Lacroix, O.R. Long, M. Olmedo Negrete, M.I. Paneva, A. Shrinivas, W. Si, L. Wang, H. Wei, S. Wimpenny, B.R. Yates

University of California, Riverside, Riverside, USA

J.G. Branson, S. Cittolin, M. Derdzinski, B. Hashemi, A. Holzner, D. Klein, G. Kole, V. Krutelyov, J. Letts, I. Macneill, M. Masciovecchio, D. Olivito, S. Padhi, M. Pieri, M. Sani, V. Sharma, S. Simon, M. Tadel, A. Vartak, S. Wasserbaech [64], J. Wood, F. Würthwein, A. Yagil, G. Zevi Della Porta

University of California, San Diego, La Jolla, USA

N. Amin, R. Bhandari, J. Bradmiller-Feld, C. Campagnari, A. Dishaw, V. Dutta, M. Franco Sevilla, C. George, F. Golf, L. Gouskos, J. Gran, R. Heller, J. Incandela, S.D. Mullin, A. Ovcharova, H. Qu, J. Richman, D. Stuart, I. Suarez, J. Yoo

University of California, Santa Barbara – Department of Physics, Santa Barbara, USA

D. Anderson, J. Bendavid, A. Bornheim, J.M. Lawhorn, H.B. Newman, T. Nguyen, C. Pena, M. Spiropulu, J.R. Vlimant, S. Xie, Z. Zhang, R.Y. Zhu

California Institute of Technology, Pasadena, USA

M.B. Andrews, T. Ferguson, T. Mudholkar, M. Paulini, J. Russ, M. Sun, H. Vogel, I. Vorobiev, M. Weinberg

Carnegie Mellon University, Pittsburgh, USA

J.P. Cumalat, W.T. Ford, F. Jensen, A. Johnson, M. Krohn, S. Leontsinis, T. Mulholland, K. Stenson, S.R. Wagner

University of Colorado Boulder, Boulder, USA

J. Alexander, J. Chaves, J. Chu, S. Dittmer, K. Mcdermott, N. Mirman, J.R. Patterson, A. Rinkevicius, A. Ryd, L. Skinnari, L. Soffi, S.M. Tan, Z. Tao, J. Thom, J. Tucker, P. Wittich, M. Zientek

Cornell University, Ithaca, USA

S. Abdullin, M. Albrow, G. Apollinari, A. Apresyan, A. Apyan, S. Banerjee, L.A.T. Bauerdick, A. Beretvas, J. Berryhill, P.C. Bhat, G. Bolla, K. Burkett, J.N. Butler, A. Canepa, G.B. Cerati, H.W.K. Cheung, F. Chlebana, M. Cremonesi, J. Duarte, V.D. Elvira, J. Freeman, Z. Gecse, E. Gottschalk, L. Gray, D. Green, S. Grünendahl, O. Gutsche, R.M. Harris, S. Hasegawa, J. Hirschauer, Z. Hu, B. Jayatilaka, S. Jindariani, M. Johnson, U. Joshi, B. Klima, B. Kreis, S. Lammel, D. Lincoln, R. Lipton, M. Liu, T. Liu, R. Lopes De Sá, J. Lykken, K. Maeshima, N. Magini, J.M. Marraffino, S. Maruyama, D. Mason, P. McBride, P. Merkel, S. Mrenna, S. Nahn, V. O'Dell, K. Pedro, O. Prokofyev, G. Rakness, L. Ristori, B. Schneider, E. Sexton-Kennedy, A. Soha, W.J. Spalding, L. Spiegel, S. Stoynev, J. Strait, N. Strobbe, L. Taylor, S. Tkaczyk, N.V. Tran, L. Uplegger, E.W. Vaandering, C. Vernieri, M. Verzocchi, R. Vidal, M. Wang, H.A. Weber, A. Whitbeck

Fermi National Accelerator Laboratory, Batavia, USA

D. Acosta, P. Avery, P. Bortignon, D. Bourilkov, A. Brinkerhoff, A. Carnes, M. Carver, D. Curry, S. Das, R.D. Field, I.K. Furic, J. Konigsberg, A. Korytov, K. Kotov, P. Ma, K. Matchev, H. Mei, G. Mitselmakher, D. Rank, D. Sperka, N. Terentyev, L. Thomas, J. Wang, S. Wang, J. Yelton

University of Florida, Gainesville, USA

Y.R. Joshi, S. Linn, P. Markowitz, J.L. Rodriguez

Florida International University, Miami, USA

A. Ackert, T. Adams, A. Askew, S. Hagopian, V. Hagopian, K.F. Johnson, T. Kolberg, G. Martinez, T. Perry, H. Prosper, A. Saha, A. Santra, R. Yohay

Florida State University, Tallahassee, USA

M.M. Baarmand, V. Bhopatkar, S. Colafranceschi, M. Hohlmann, D. Noonan, T. Roy, F. Yumiceva

Florida Institute of Technology, Melbourne, USA

M.R. Adams, L. Apanasevich, D. Berry, R.R. Betts, R. Cavanaugh, X. Chen, O. Evdokimov, C.E. Gerber, D.A. Hangal, D.J. Hofman, K. Jung, J. Kamin, I.D. Sandoval Gonzalez, M.B. Tonjes, H. Trauger, N. Varelas, H. Wang, Z. Wu, J. Zhang

University of Illinois at Chicago (UIC), Chicago, USA

B. Bilki [65], W. Clarida, K. Dilsiz [66], S. Durgut, R.P. Gandrajula, M. Haytmyradov, V. Khristenko, J.-P. Merlo, H. Mermerkaya [67], A. Mestvirishvili, A. Moeller, J. Nachtman, H. Ogul [68], Y. Onel, F. Ozok [69], A. Penzo, C. Snyder, E. Tiras, J. Wetzel, K. Yi

The University of Iowa, Iowa City, USA

B. Blumenfeld, A. Cocoros, N. Eminizer, D. Fehling, L. Feng, A.V. Gritsan, P. Maksimovic, J. Roskes, U. Sarica, M. Swartz, M. Xiao, C. You

Johns Hopkins University, Baltimore, USA

A. Al-bataineh, P. Baringer, A. Bean, S. Boren, J. Bowen, J. Castle, S. Khalil, A. Kropivnitskaya, D. Majumder, W. Mcbrayer, M. Murray, C. Royon, S. Sanders, E. Schmitz, R. Stringer, J.D. Tapia Takaki, Q. Wang

The University of Kansas, Lawrence, USA

A. Ivanov, K. Kaadze, Y. Maravin, A. Mohammadi, L.K. Saini, N. Skhirtladze, S. Toda

Kansas State University, Manhattan, USA

F. Rebassoo, D. Wright

Lawrence Livermore National Laboratory, Livermore, USA

C. Anelli, A. Baden, O. Baron, A. Belloni, B. Calvert, S.C. Eno, C. Ferraioli, N.J. Hadley, S. Jabeen, G.Y. Jeng, R.G. Kellogg, J. Kunkle, A.C. Mignerey, F. Ricci-Tam, Y.H. Shin, A. Skuja, S.C. Tonwar

University of Maryland, College Park, USA

D. Abercrombie, B. Allen, V. Azzolini, R. Barbieri, A. Baty, R. Bi, S. Brandt, W. Busza, I.A. Cali, M. D'Alfonso, Z. Demiragli, G. Gomez Ceballos, M. Goncharov, D. Hsu, Y. Iiyama, G.M. Innocenti, M. Klute, D. Kovalskyi, Y.S. Lai, Y.-J. Lee, A. Levin, P.D. Luckey, B. Maier, A.C. Marini, C. Mcginn, C. Mironov, S. Narayanan, X. Niu, C. Paus, C. Roland, G. Roland, J. Salfeld-Nebgen, G.S.F. Stephans, K. Tatar, D. Velicanu, J. Wang, T.W. Wang, B. Wyslouch

Massachusetts Institute of Technology, Cambridge, USA

A.C. Benvenuti, R.M. Chatterjee, A. Evans, P. Hansen, S. Kalafut, Y. Kubota, Z. Lesko, J. Mans, S. Nourbakhsh, N. Ruckstuhl, R. Rusack, J. Turkewitz

University of Minnesota, Minneapolis, USA

J.G. Acosta, S. Oliveros

University of Mississippi, Oxford, USA

E. Avdeeva, K. Bloom, D.R. Claes, C. Fangmeier, R. Gonzalez Suarez, R. Kamalieddin, I. Kravchenko, J. Monroy, J.E. Siado, G.R. Snow, B. Stieger

University of Nebraska-Lincoln, Lincoln, USA

M. Alyari, J. Dolen, A. Godshalk, C. Harrington, I. Iashvili, D. Nguyen, A. Parker, S. Rappoccio, B. Roozbahani

State University of New York at Buffalo, Buffalo, USA

G. Alverson, E. Barberis, A. Hortiangtham, A. Massironi, D.M. Morse, D. Nash, T. Orimoto, R. Teixeira De Lima, D. Trocino, D. Wood

Northeastern University, Boston, USA

S. Bhattacharya, O. Charaf, K.A. Hahn, N. Mucia, N. Odell, B. Pollack, M.H. Schmitt, K. Sung, M. Trovato, M. Velasco

Northwestern University, Evanston, USA

N. Dev, M. Hildreth, K. Hurtado Anampa, C. Jessop, D.J. Karmgard, N. Kellams, K. Lannon, N. Loukas, N. Marinelli, F. Meng, C. Mueller, Y. Musienko [35], M. Planer, A. Reinsvold, R. Ruchti, G. Smith, S. Taroni, M. Wayne, M. Wolf, A. Woodard

University of Notre Dame, Notre Dame, USA

J. Alimena, L. Antonelli, B. Bylsma, L.S. Durkin, S. Flowers, B. Francis, A. Hart, C. Hill, W. Ji, B. Liu, W. Luo, D. Puigh, B.L. Winer, H.W. Wulsin

The Ohio State University, Columbus, USA

A. Benaglia, S. Cooperstein, O. Driga, P. Elmer, J. Hardenbrook, P. Hebda, S. Higginbotham, D. Lange, J. Luo, D. Marlow, K. Mei, I. Ojalvo, J. Olsen, C. Palmer, P. Piroué, D. Stickland, C. Tully

Princeton University, Princeton, USA

S. Malik, S. Norberg

University of Puerto Rico, Mayaguez, USA

A. Barker, V.E. Barnes, S. Folgueras, L. Gutay, M.K. Jha, M. Jones, A.W. Jung, A. Khatiwada, D.H. Miller, N. Neumeister, C.C. Peng, J.F. Schulte, J. Sun, F. Wang, W. Xie

Purdue University, West Lafayette, USA

T. Cheng, N. Parashar, J. Stupak

Purdue University Northwest, Hammond, USA

A. Adair, B. Akgun, Z. Chen, K.M. Ecklund, F.J.M. Geurts, M. Guilbaud, W. Li, B. Michlin, M. Northup, B.P. Padley, J. Roberts, J. Rorie, Z. Tu, J. Zabel

Rice University, Houston, USA

A. Bodek, P. de Barbaro, R. Demina, Y.t. Duh, T. Ferbel, M. Galanti, A. Garcia-Bellido, J. Han, O. Hindrichs, A. Khukhunaishvili, K.H. Lo, P. Tan, M. Verzetti

University of Rochester, Rochester, USA

R. Ciesielski, K. Goulianos, C. Mesropian

The Rockefeller University, New York, USA

A. Agapitos, J.P. Chou, Y. Gershtein, T.A. Gómez Espinosa, E. Halkiadakis, M. Heindl, E. Hughes, S. Kaplan, R. Kunnawalkam Elayavalli, S. Kyriacou, A. Lath, R. Montalvo, K. Nash, M. Osherson, H. Saka, S. Salur, S. Schnetzer, D. Sheffield, S. Somalwar, R. Stone, S. Thomas, P. Thomassen, M. Walker

Rutgers, The State University of New Jersey, Piscataway, USA

A.G. Delannoy, M. Foerster, J. Heideman, G. Riley, K. Rose, S. Spanier, K. Thapa

University of Tennessee, Knoxville, USA

O. Bouhali [70], A. Castaneda Hernandez [70], A. Celik, M. Dalchenko, M. De Mattia, A. Delgado, S. Dildick, R. Eusebi, J. Gilmore, T. Huang, T. Kamon [71], R. Mueller, Y. Pakhotin, R. Patel, A. Perloff, L. Perniè, D. Rathjens, A. Safonov, A. Tatarinov, K.A. Ulmer

Texas A&M University, College Station, USA

N. Akchurin, J. Damgov, F. De Guio, P.R. Dudero, J. Faulkner, E. Gurpinar, S. Kunori, K. Lamichhane, S.W. Lee, T. Libeiro, T. Peltola, S. Undleeb, I. Volobouev, Z. Wang

Texas Tech University, Lubbock, USA

S. Greene, A. Gurrola, R. Janjam, W. Johns, C. Maguire, A. Melo, H. Ni, P. Sheldon, S. Tuo, J. Velkovska, Q. Xu

Vanderbilt University, Nashville, USA

M.W. Arenton, P. Barria, B. Cox, R. Hirosky, A. Ledovskoy, H. Li, C. Neu, T. Sinthuprasith, X. Sun, Y. Wang, E. Wolfe, F. Xia

University of Virginia, Charlottesville, USA

R. Harr, P.E. Karchin, J. Sturdy, S. Zaleski

Wayne State University, Detroit, USA

M. Brodski, J. Buchanan, C. Caillol, S. Dasu, L. Dodd, S. Duric, B. Gomber, M. Grothe, M. Herndon, A. Hervé, U. Hussain, P. Klabbers, A. Lanaro, A. Levine, K. Long, R. Loveless, G.A. Pierro, G. Polese, T. Ruggles, A. Savin, N. Smith, W.H. Smith, D. Taylor, N. Woods

University of Wisconsin – Madison, Madison, WI, USA

† Deceased.
[1] Also at Vienna University of Technology, Vienna, Austria.
[2] Also at State Key Laboratory of Nuclear Physics and Technology, Peking University, Beijing, China.
[3] Also at Universidade Estadual de Campinas, Campinas, Brazil.
[4] Also at Universidade Federal de Pelotas, Pelotas, Brazil.
[5] Also at Université Libre de Bruxelles, Bruxelles, Belgium.
[6] Also at Institute for Theoretical and Experimental Physics, Moscow, Russia.
[7] Also at Joint Institute for Nuclear Research, Dubna, Russia.
[8] Now at Ain Shams University, Cairo, Egypt.
[9] Now at British University in Egypt, Cairo, Egypt.
[10] Also at Zewail City of Science and Technology, Zewail, Egypt.
[11] Also at Université de Haute Alsace, Mulhouse, France.
[12] Also at Skobeltsyn Institute of Nuclear Physics, Lomonosov Moscow State University, Moscow, Russia.
[13] Also at Tbilisi State University, Tbilisi, Georgia.
[14] Also at CERN, European Organization for Nuclear Research, Geneva, Switzerland.
[15] Also at RWTH Aachen University, III. Physikalisches Institut A, Aachen, Germany.
[16] Also at University of Hamburg, Hamburg, Germany.
[17] Also at Brandenburg University of Technology, Cottbus, Germany.
[18] Also at Institute of Nuclear Research ATOMKI, Debrecen, Hungary.
[19] Also at MTA-ELTE Lendület CMS Particle and Nuclear Physics Group, Eötvös Loránd University, Budapest, Hungary.
[20] Also at Institute of Physics, University of Debrecen, Debrecen, Hungary.
[21] Also at Indian Institute of Technology Bhubaneswar, Bhubaneswar, India.
[22] Also at Institute of Physics, Bhubaneswar, India.
[23] Also at University of Visva-Bharati, Santiniketan, India.
[24] Also at University of Ruhuna, Matara, Sri Lanka.
[25] Also at Isfahan University of Technology, Isfahan, Iran.
[26] Also at Yazd University, Yazd, Iran.
[27] Also at Plasma Physics Research Center, Science and Research Branch, Islamic Azad University, Tehran, Iran.
[28] Also at Università degli Studi di Siena, Siena, Italy.
[29] Also at INFN Sezione di Milano-Bicocca; Università di Milano-Bicocca, Milano, Italy.
[30] Also at Purdue University, West Lafayette, USA.
[31] Also at International Islamic University of Malaysia, Kuala Lumpur, Malaysia.
[32] Also at Malaysian Nuclear Agency, MOSTI, Kajang, Malaysia.
[33] Also at Consejo Nacional de Ciencia y Tecnología, Mexico city, Mexico.
[34] Also at Warsaw University of Technology, Institute of Electronic Systems, Warsaw, Poland.

[35] Also at Institute for Nuclear Research, Moscow, Russia.
[36] Now at National Research Nuclear University 'Moscow Engineering Physics Institute' (MEPhI), Moscow, Russia.
[37] Also at St. Petersburg State Polytechnical University, St. Petersburg, Russia.
[38] Also at University of Florida, Gainesville, USA.
[39] Also at P.N. Lebedev Physical Institute, Moscow, Russia.
[40] Also at California Institute of Technology, Pasadena, USA.
[41] Also at Budker Institute of Nuclear Physics, Novosibirsk, Russia.
[42] Also at Faculty of Physics, University of Belgrade, Belgrade, Serbia.
[43] Also at INFN Sezione di Roma; Sapienza Università di Roma, Rome, Italy.
[44] Also at University of Belgrade, Faculty of Physics and Vinca Institute of Nuclear Sciences, Belgrade, Serbia.
[45] Also at Scuola Normale e Sezione dell'INFN, Pisa, Italy.
[46] Also at National and Kapodistrian University of Athens, Athens, Greece.
[47] Also at Riga Technical University, Riga, Latvia.
[48] Also at Universität Zürich, Zurich, Switzerland.
[49] Also at Stefan Meyer Institute for Subatomic Physics (SMI), Vienna, Austria.
[50] Also at Istanbul University, Faculty of Science, Istanbul, Turkey.
[51] Also at Adiyaman University, Adiyaman, Turkey.
[52] Also at Istanbul Aydin University, Istanbul, Turkey.
[53] Also at Mersin University, Mersin, Turkey.
[54] Also at Cag University, Mersin, Turkey.
[55] Also at Piri Reis University, Istanbul, Turkey.
[56] Also at Izmir Institute of Technology, Izmir, Turkey.
[57] Also at Necmettin Erbakan University, Konya, Turkey.
[58] Also at Marmara University, Istanbul, Turkey.
[59] Also at Kafkas University, Kars, Turkey.
[60] Also at Istanbul Bilgi University, Istanbul, Turkey.
[61] Also at Rutherford Appleton Laboratory, Didcot, United Kingdom.
[62] Also at School of Physics and Astronomy, University of Southampton, Southampton, United Kingdom.
[63] Also at Instituto de Astrofísica de Canarias, La Laguna, Spain.
[64] Also at Utah Valley University, Orem, USA.
[65] Also at Beykent University, Istanbul, Turkey.
[66] Also at Bingol University, Bingol, Turkey.
[67] Also at Erzincan University, Erzincan, Turkey.
[68] Also at Sinop University, Sinop, Turkey.
[69] Also at Mimar Sinan University, Istanbul, Istanbul, Turkey.
[70] Also at Texas A&M University at Qatar, Doha, Qatar.
[71] Also at Kyungpook National University, Daegu, Korea.